

1-1-2022

Synthesis of novel oxadiazole derivatives and their cytotoxic activity against various cancer cell lines

BİLGESU ONUR SUCU

ELİF BEYZA KOÇ

Follow this and additional works at: <https://journals.tubitak.gov.tr/chem>

 Part of the [Chemistry Commons](#)



Recommended Citation

SUCU, BİLGESU ONUR and KOÇ, ELİF BEYZA (2022) "Synthesis of novel oxadiazole derivatives and their cytotoxic activity against various cancer cell lines," *Turkish Journal of Chemistry*. Vol. 46: No. 4, Article 13. <https://doi.org/10.55730/1300-0527.3417>

Available at: <https://journals.tubitak.gov.tr/chem/vol46/iss4/13>

This Article is brought to you for free and open access by TÜBİTAK Academic Journals. It has been accepted for inclusion in Turkish Journal of Chemistry by an authorized editor of TÜBİTAK Academic Journals. For more information, please contact academic.publications@tubitak.gov.tr.

Synthesis of novel oxadiazole derivatives and their cytotoxic activity against various cancer cell lines

Bilgesu Onur SUCU^{1,2,*} , Elif Beyza KOÇ¹ 

¹Research Institute for Health Sciences and Technologies (SABITA), Center of Drug Discovery and Development, İstanbul Medipol University, İstanbul, Turkey

²Department of Medical Services and Techniques, Vocational School of Health Services, İstanbul Medipol University, İstanbul, Turkey

Received: 13.01.2022 • Accepted/Published Online: 12.03.2022 • Final Version: 05.08.2022

Abstract: Caffeic acid (CA), ferulic acid (FA) and caffeic acid phenethyl ester (CAPE) have a broad anticancer effect on various cell lines. In this study, nine ferulic and caffeic acid-based 1,2,4 and 1,3,4 oxadiazole molecular hybrids were synthesized and their cytotoxic activity was evaluated mainly against Glioblastoma (GBM) cell lines. Compounds **1** and **5** exhibited the highest inhibitory activity against three different GBM cell lines (LN229, T98G, and U87), without toxicity to healthy human mesenchymal stem cells (hMSC). In addition, their cytotoxicity was also evaluated against three additional cancer cell lines and more inhibitory results were found than GBM cell lines. The IC₅₀ values of compound **5** in U87, T98G, LN229, SKOV3, MCF7, and A549 cells were determined as 35.1, 34.4, 37.9, 14.2, 30.9, and 18.3 μ M. In the light of biological activity studies, the developed compounds have a high potential to lead studies for the development of new drug candidates for the treatment of cancer.

Key words: 1,2,4-Oxadiazoles, 1,3,4-Oxadiazoles, anticancer activity, glioblastoma cancer cells

1. Introduction

Glioblastoma (GBM) is a very common and aggressive type of primary brain tumor in adults and it was classified as a grade IV glioma tumor by World Health Organization (WHO) [1–3]. Current treatment options such as radiotherapy, chemotherapy, and surgical resection do not increase the survival rate of the patients [4,5]. Temozolomide (3,4-dihydro-3-methyl-4-oxoimidazo-[5,1-d]-1,2,3,5-tetrazine-8-carboxamide, TMZ) has been employed for GBM treatment [6,7]. Since it has a low molecular weight, it could easily pass the blood-brain barrier [8]. In recent years, a combination of TMZ with radiotherapy has been used as standard therapy [9]. However, no further improvement has been noted with TMZ, since some GBM patients are resistant to TMZ treatment [10]. Therefore urgently new therapeutic agents are needed in this area.

Caffeic acid (CA), ferulic acid (FA), and caffeic acid phenethyl ester (CAPE) are biologically active phenolic compounds (Figure 1). While CA and FA are found in many agricultural products such as fruits and vegetables [11–13], CAPE is obtained from propolis in honey bee hives. Their various biological activities have been reported such as antioxidant, antimicrobial, antiinflammatory, and anticancer [14–18]. The phenylpropanoid scaffold of caffeic acid is widely utilized to develop novel biologically active compounds [19]. The oxadiazole core mimicking carboxylic acids, esters and amides can be used as their bioisosters [20]. They also display a wide range of biological and pharmacological activities including antimycobacterial [21,22], analgesic [23], antidepressant [24], COX-2 inhibitors [25], and anticancer [26]. Many of the 1,2,4-oxadiazoles and 1,3,4-oxadiazole compounds are being investigated in biological screening. Due to the potential activities of these compounds, interest towards them is increasing and the acquired data is gaining significance. In our previous study, we synthesized some amides and heterocyclic derivatives and found that the 1,2,4-oxadiazole analog was more potent than the others [27]. Therefore, in this study, we aimed to synthesize some novel hybrid molecules carrying oxadiazoles (Figure 1) and to investigate their anticancer activities against various cancer cell lines.

2. Materials and methods

2.1. Chemistry

All the chemicals and reagents were purchased from Merck, Sigma-Aldrich, TCI. The purity of the compounds was checked on thin layer chromatography (TLC). Column chromatography purifications were performed on Merck Silica gel

* Correspondence: bsucu@medipol.edu.tr

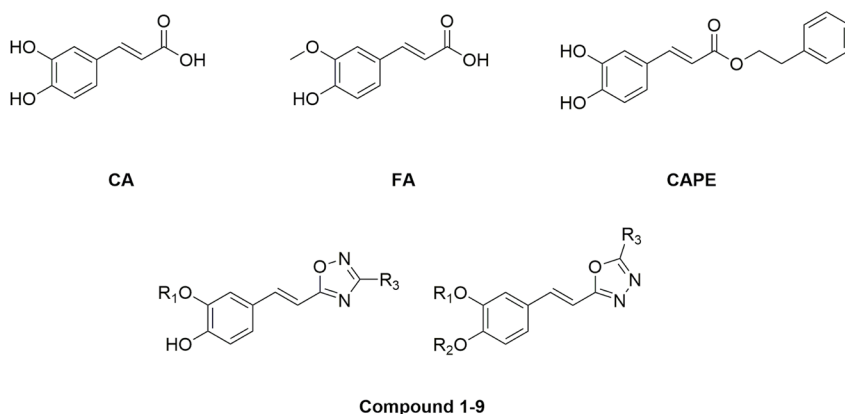


Figure 1. Structures of caffeic acid (CA), ferulic acid (FA), caffeic acid phenethyl ester (CAPE), and Compound 1-9.

60. Melting points were taken in open capillary tubes using a Stuart SMP30. High resolution mass spectrum (HRMS) was measured using Thermo ORBITRAP Q-EXACTIVE instrument. The ^1H and ^{13}C (APT) NMR spectra were measured in CDCl_3 , CD_3OD , or $\text{DMSO}-d_6$ on a Varian NMR 500 MHz NMR spectrophotometer.

2.1.1. General procedure for the synthesis of 3,5-disubstitue-1,2,4-oxadiazole derivatives (1-3)

The mixture of 3,4-Dihydroxyhydrocinnamic acid or ferulic acid (1 mmol), benzamide oxime or 4-(trifluoromethyl) benzamidoxime (1.1 mmol), EDC.HCl (1.2 mmol), and HOBT (1.2 mmol) were stirred in DMF (5 mL). After 1 h, the reaction mixture was heated and stirred overnight at 140°C . The mixture was cooled to r.t., quenched with LiCl solution and extracted with excess EtOAc. The organic phase dried with Na_2SO_4 . It was purified by column chromatography with EtOAc:*n*-hexane (1:2) mixture.

2.1.2. General procedure for the synthesis of 2,5-disubstitue-1,3,4-oxadiazole derivatives (4-9)

An equimolar mixture of corresponding hydrazide (1 mmol) with caffeic acid/ferulic acid (1 mmol) was refluxed with phosphorus oxychloride (1 mL) for 2–3 h at 100°C . Reaction mixture was cooled to room temperature and poured into ice cold water. The precipitate obtained was filtered off, washed with water. It was purified by column chromatography with EtOAc:*n*-hexane (1:1) mixture.

2.1.3. Spectral data of the compounds 1-9

2-Methoxy-4-(2-(3-phenyl-1,2,4-oxadiazol-5-yl)vinyl)phenol (1)

Light yellow solid. Yield: 68%; mp: $166\text{--}168^\circ\text{C}$. R_f : 0.56 (1:1.5 EtOAc:*n*-hexane). ^1H NMR (500 MHz, CDCl_3) δ (ppm): 8.15–8.09 (m, 2H), 7.80 (d, $J = 16.3$ Hz, 1H), 7.53–7.45 (m, 3H), 7.15 (dd, $J = 8.2, 2.0$ Hz, 1H), 7.09 (d, $J = 2.0$ Hz, 1H), 6.96 (d, $J = 8.1$ Hz, 1H), 6.90 (d, $J = 16.3$ Hz, 1H), 3.93 (s, 3H). ^{13}C NMR (APT) (125 MHz, CDCl_3) δ (ppm): 175.68, 168.70, 148.37, 147.07, 142.89, 131.23, 128.95, 127.57, 127.12, 127.08, 123.12, 115.05, 109.28, 107.69, 56.06. HRMS (m/z): $[\text{M}-\text{H}]^-$ calculated for $\text{C}_{17}\text{H}_{14}\text{N}_2\text{O}_3$: 293.0926; found: 293.0932.

4-(2-(3-(4-(Trifluoromethyl)phenyl)-1,2,4-oxadiazol-5-yl)vinyl)benzene-1,2-diol (2)

Light yellow solid. Yield: 64%; mp: $223\text{--}225^\circ\text{C}$. R_f : 0.48 (1:1 EtOAc:*n*-hexane). ^1H NMR (500 MHz, CD_3OD) δ (ppm): 8.27 (d, $J = 8.2$ Hz, 2H), 7.84 (d, $J = 8.2$ Hz, 2H), 7.81 (d, $J = 16.2$ Hz, 1H), 7.16 (d, $J = 2.1$ Hz, 1H), 7.07 (dd, $J = 8.1, 2.1$ Hz, 1H), 6.95 (d, $J = 16.3$ Hz, 1H), 6.83 (d, $J = 8.1$ Hz, 1H). ^{13}C NMR (APT) (125 MHz, CD_3OD) δ (ppm): 176.70, 167.29, 148.63, 145.62, 143.88, 132.27, 130.72, 127.55, 126.40, 125.60, 125.02, 122.85, 121.73, 115.21, 113.62, 105.67. HRMS (m/z): $[\text{M}-\text{H}]^-$ calculated for $\text{C}_{17}\text{H}_{11}\text{F}_3\text{N}_2\text{O}_3$: 347.0644; found: 347.0649.

2-Methoxy-4-(2-(3-(4-(trifluoromethyl)phenyl)-1,2,4-oxadiazol-5-yl)vinyl)phenol (3)

White solid. Yield: 60%; mp: 162°C . R_f : 0.68 (1:1.5 EtOAc:*n*-hexane). ^1H NMR (500 MHz, CDCl_3) δ (ppm): 8.24 (d, $J = 8.1$ Hz, 2H), 7.82 (d, $J = 16.3$ Hz, 1H), 7.76 (d, $J = 8.2$ Hz, 2H), 7.17 (dd, $J = 8.2, 2.0$ Hz, 1H), 7.10 (d, $J = 1.9$ Hz, 1H), 6.97 (d, $J = 8.2$ Hz, 1H), 6.90 (d, $J = 16.3$ Hz, 1H), 6.01 (s, 1H), 3.96 (s, 3H). ^{13}C NMR (APT) (125 MHz, CDCl_3) δ (ppm): 176.03, 167.60, 148.40, 146.95, 143.26, 132.66, 130.45, 127.77, 126.89, 125.85, 124.88, 123.15, 122.72, 114.97, 109.18, 107.29, 55.98. HRMS (m/z): $[\text{M}-\text{H}]^-$ calculated for $\text{C}_{18}\text{H}_{13}\text{F}_3\text{N}_2\text{O}_3$: 361.0807; found: 361.0807.

4-(2-(5-Phenyl-1,3,4-oxadiazol-2-yl)vinyl)benzene-1,2-diol (4)

Yellow-brown solid. Yield: 62%; mp: 210°C decompose, R_f : 0.68 (2:1 EtOAc:*n*-hexane). ^1H NMR (500 MHz, $\text{DMSO}-d_6$) δ (ppm): 8.10–8.07 (m, 2H), 7.63–7.56 (m, 4H), 7.16 (d, $J = 2.1$ Hz, 1H), 7.09 (dd, $J = 8.2, 2.1$ Hz, 1H), 6.99 (d, $J = 16.3$

H_z, 1H), 6.82 (d, *J* = 8.1 Hz, 1H). ¹³C NMR (APT) (125 MHz, DMSO-*d*₆) δ (ppm): 164.48, 162.92, 148.01, 145.66, 139.67, 131.86, 129.39, 126.55, 126.25, 123.47, 120.64, 115.91, 114.58, 105.95. HRMS (m/z): [M+H]⁺ calculated for C₁₆H₁₂N₂O₃: 281.0926; found: 281.0911, [M+Na]⁺ calculated for C₁₆H₁₂N₂O₃: 303.0746 found: 303.0729.

4-(2-(5-(Furan-2-yl)-1,3,4-oxadiazol-2-yl)vinyl)benzene-1,2-diol (5)

Yellow-brown solid. Yield: 62%; mp: 210 °C decompose, R_f: 0.46 (3:1 EtOAc:*n*-hexane). ¹H NMR (500 MHz, CD₃OD) δ (ppm): 7.85 (d, *J* = 1.7 Hz, 1H), 7.55 (d, *J* = 16.3 Hz, 1H), 7.32 (d, *J* = 3.5 Hz, 1H), 7.14–7.11 (m, 1H), 7.01 (dd, *J* = 8.1, 1.7 Hz, 1H), 6.87 (d, *J* = 16.3 Hz, 1H), 6.81 (d, *J* = 8.2 Hz, 1H), 6.73 (dd, *J* = 3.5, 1.8 Hz, 1H). ¹³C NMR (APT) (125 MHz, CD₃OD) δ (ppm): 165.87, 158.05, 149.59, 147.86, 147.00, 142.04, 140.43, 128.03, 122.56, 116.60, 115.69, 114.67, 113.48, 106.10. HRMS (m/z): [M+H]⁺ calculated for C₁₄H₁₀N₂O₄: 271.0719; found: 271.0704.

2-Methoxy-5-(2-(5-phenyl-1,3,4-oxadiazol-2-yl)vinyl)phenol (6)

White solid. Yield: 50%; mp: 164–166 °C. R_f: 0.62 (2:1 EtOAc:*n*-hexane). ¹H NMR (500 MHz, CDCl₃) δ (ppm): 8.13–8.10 (m, 2H), 7.56–7.50 (m, *J* = 12.7, 6.8, 3.9 Hz, 4H), 7.22 (d, *J* = 2.1 Hz, 1H), 7.08 (dd, *J* = 8.3, 2.1 Hz, 1H), 6.95 (d, *J* = 16.3 Hz, 1H), 6.89 (d, *J* = 8.3 Hz, 1H), 3.94 (s, 3H). ¹³C NMR (APT) (125 MHz, CDCl₃) δ (ppm): 164.68, 164.00, 148.45, 146.19, 138.88, 131.79, 129.20, 128.65, 127.07, 124.10, 121.15, 112.79, 110.86, 108.30, 56.19. HRMS (m/z): [M+H]⁺ calculated for C₁₇H₁₄N₂O₃: 295.1083; found: 295.1068.

5-(2-(5-(Furan-2-yl)-1,3,4-oxadiazol-2-yl)vinyl)-2-methoxyphenol (7)

White solid. Yield: 50%; mp: 166–168 °C. R_f: 0.57 (2:1 EtOAc:*n*-hexane). ¹H NMR (500 MHz, CDCl₃) δ (ppm): 7.66 (dd, *J* = 1.7, 0.6 Hz, 1H), 7.53 (d, *J* = 16.4 Hz, 1H), 7.21 (dd, *J* = 3.5, 0.6 Hz, 1H), 7.19 (d, *J* = 2.1 Hz, 1H), 7.08 (dd, *J* = 8.3, 2.1 Hz, 1H), 6.92 (d, *J* = 16.3 Hz, 1H), 6.88 (d, *J* = 8.3 Hz, 1H), 6.62 (dd, *J* = 3.5, 1.8 Hz, 1H), 3.94 (s, 3H). ¹³C NMR (APT) (125 MHz, CDCl₃) δ (ppm): 164.06, 156.85, 148.49, 146.17, 145.81, 139.74, 139.26, 128.56, 121.23, 114.15, 112.76, 112.36, 110.84, 107.82, 56.20. HRMS (m/z): [M+H]⁺ calculated for C₁₅H₁₂N₂O₄: 285.0875; found: 285.0860.

2-Methoxy-4-(2-(5-phenyl-1,3,4-oxadiazol-2-yl)vinyl)phenol (8)

Yellow solid. Yield: 56%; mp: 120–124 °C. R_f: 0.57 (2:1 EtOAc:*n*-hexane). ¹H NMR (500 MHz, CD₃OD) δ (ppm): 8.11–8.08 (m, 2H), 7.65 (d, *J* = 16.3 Hz, 1H), 7.61–7.57 (m, 3H), 7.25 (d, *J* = 2.0 Hz, 1H), 7.13 (dd, *J* = 8.2, 2.0 Hz, 1H), 6.94 (d, *J* = 16.3 Hz, 1H), 6.81 (d, *J* = 8.2 Hz, 1H), 3.92 (s, 3H). ¹³C NMR (APT) (125 MHz, CD₃OD) δ (ppm): 166.75, 165.13, 152.95, 150.17, 142.10, 133.10, 130.38, 130.22, 127.83, 126.82, 124.86, 124.12, 117.12, 111.05, 105.73, 56.37. HRMS (m/z): [M+H]⁺ calculated for C₁₇H₁₄N₂O₃: 295.1083; found: 295.1068.

4-(2-(5-(Furan-2-yl)-1,3,4-oxadiazol-2-yl)vinyl)-2-methoxyphenol (9)

Yellow solid. Yield: 52%; mp: 178–180 °C. R_f: 0.61 (2:1 EtOAc:*n*-hexane). ¹H NMR (500 MHz, CD₃OD) δ (ppm): 7.87 (dd, *J* = 1.2 Hz, 1H), 7.62 (d, *J* = 16.3 Hz, 1H), 7.33 (d, *J* = 3.4 Hz, 1H), 7.25 (d, *J* = 1.9 Hz, 1H), 7.13 (dd, *J* = 8.2, 1.9 Hz, 1H), 6.95 (d, *J* = 16.3 Hz, 1H), 6.81 (d, *J* = 8.2 Hz, 1H), 6.75 (dd, *J* = 3.5, 1.8 Hz, 1H), 3.92 (s, 3H). ¹³C NMR (APT) (125 MHz, CD₃OD) δ (ppm): 166.10, 157.96, 150.22, 147.81, 142.31, 140.50, 126.72, 124.21, 117.14, 115.58, 113.46, 111.04, 105.36, 56.37. HRMS (m/z): [M+H]⁺ calculated for C₁₅H₁₂N₂O₄: 285.0875; found: 285.0859. [M+Na]⁺ calculated for C₁₅H₁₂N₂O₄: 307.0694 found: 307.0678.

2.2. Biological methods

LN229-GBM (ATCC, CRL-2611), T98G (ATTC, CRL-1690), U87 (ATCC, HTB-14), MCF7 (ATCC, HTB-22), SKOV3 (ATCC, HTB-77), A549 (ATCC, CCL-185) and Primary Human Mesenchymal Stem (hMSC) (UE7T-13 cells no. RBRC-RCB2161; RIKEN, Japan) cells were available in our laboratory. In vitro experiments were conducted using Gibco brand fetal bovine serum (FBS), high and low glucose Dulbecco's Modified Eagle Medium (DMEM), Penicillin-Streptomycin, L-Glutamine, and Trypsin/EDTA 0.25%. Cytotoxicity assays were performed using the Promega brand CellTiter-Glo[®] Luminescent Cell Viability Assay (Cat. no. #G7572) and the Corning 96-black plate (Cat. no. #3603).

2.2.1. Cell culture

LN229, T98G, U87, MCF7, SKOV3, and A549 cell lines were used for cell viability. Cancer cell lines were grown with high glucose Dulbecco's Modified Eagle (DMEM) containing 10% FBS, 1% Penicillin-Streptomycin, and 1% L-Glutamine at 37 °C in a 5% CO₂ incubator. The cells were grown on a 10 cm (Corning) petri dish. The effect of the most active molecule on the cancer cell line on the healthy cell line was investigated using hMSC cells. hMSC cells were cultured on a 10 cm petri dish with low glucose DMEM medium containing 10% FBS, 1% Penicillin-Streptomycin, and 1% L-Glutamine at 37 °C in a 5% CO₂ incubator. Then, to perform cell viability analysis, the cells were removed from the flask with 0.25% trypsin/EDTA. LN229, T98G, U87, MCF7, SKOV3, A549, and hMSC cells were seeded into 96-well black plate at a density of 6 × 10³, 5.5 × 10³, 6 × 10³, 6.5 × 10³, 7.5 × 10³, 6.5 × 10³, and 6.5 × 10³ cells per well, respectively.

2.2.2. Analysis of cell viability

Cells were seeded in 96-well black plates and incubated for 24 h at 37 °C in 5% CO₂. The culture medium was removed and the cells were treated for 48 h in three different wells for each concentration (1, 10, 25, 50, 100, 250 μM) of CA, CAPE,

and novel oxadiazole derivatives. Cell Titer-Glo reagent was added to each well after 48 h of treatment, and samples were analyzed on Spectramax (SpectraMax i3x Multi-Mode Detection Platform). Results were standardized relative to cell controls treated with the highest dose (0.1%) of the compound's solvent, dimethyl sulfoxide (DMSO) (Santa Cruz). IC_{50} values were determined using GraphPad 8.0.2.

2.2.3. Statistical analysis

Experiments were carried out in three sets, each with its own set of results, which were expressed as mean standard error. All statistical comparisons were made using the Student's t-test, which claimed equal variance. At * p 0.05 and ** p 0.01, the differences were declared statistically significant. The data was expressed as a standard error of the mean (SEM).

3. Results and discussion

3.1. Chemistry

A recent study published by Tripathi et al., showed that the similar hybrid molecules can be effective not only on cancer cells, also used against Alzheimer's disease (AD) [28]. The inhibition of BACE-1 enzyme with our compound **8** was reported here as a therapeutic approach to treat AD. In our study, the cytotoxic activity of same compound and additional some new oxadiazoles were evaluated as well. In view of this point, some novel 1,2,4- and 1,3,4-oxadiazole analogues (**1-9**) were prepared by one-pot reactions (Figure 2). The 3,5-disubstituted-1,2,4-oxadiazoles (**1-3**) were obtained by the reaction of caffeic/ferulic acid and the corresponding oxime in the presence of EDC and HOBT. Since we used commercially available trans isomers of caffeic/ferulic acids as starting material, only same isomer was obtained at the end of our method. Compound **1** was synthesized for cytotoxic activity comparison with our previous work [27]. To clarify, the effect of the $-CF_3$ group on phenyl moiety, compounds **2** and **3** were prepared and compared their activity with compound **1**. The 2,5-disubstituted-1,3,4-oxadiazoles (**4-9**) were synthesized to investigate the effect of 1,3,4-oxadiazole ring. These compounds were obtained by the reaction of hydrazide and caffeic/ferulic acid with $POCl_3$. The synthesis of the compounds was achieved in 50%–68% yield. Following the synthesis, the crude mixtures were purified by column chromatography and PLC methods using silica gel. All compounds were characterized via 1H NMR and ^{13}C NMR (APT). Furthermore, calculated and measured m/z values of the compounds were also found compatible in HRMS analysis.

3.2. Biological

Anticancer activity of the synthesized novel oxadiazole derivatives were evaluated against on U87, T98G, and LN229 GBM cell lines. The various concentrations of the derivatives were used to determine IC_{50} values (Table 1) of each compound against the selected cell lines. Among the compounds having 1,2,4-oxadiazole ring, compound **1**, exhibited most potent activity on the selected GBM cancer cell lines. On the other hand, among the 1,3,4-oxadiazoles, compound **5** showed the lowest IC_{50} (Figure 3).

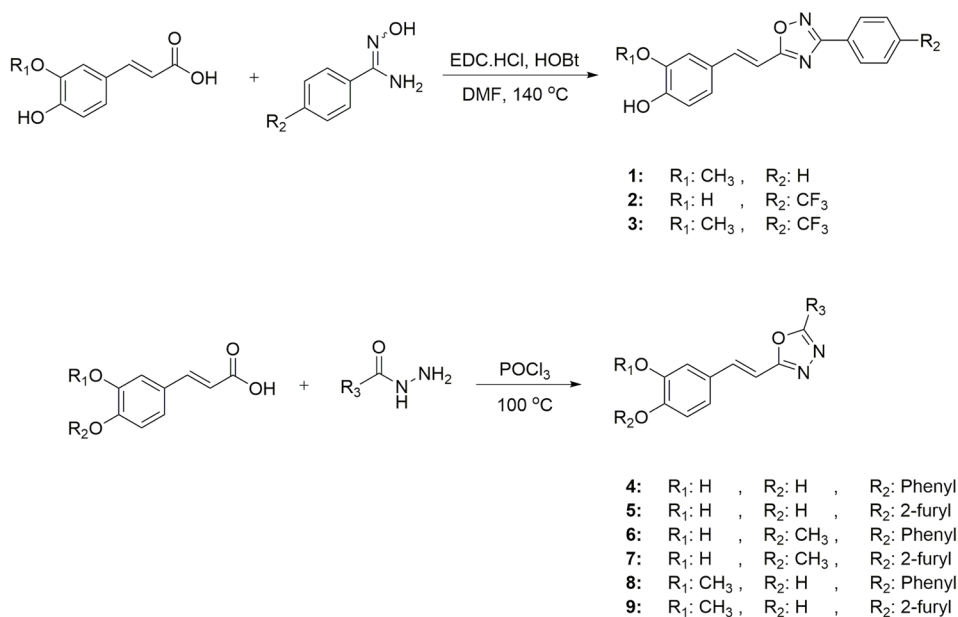
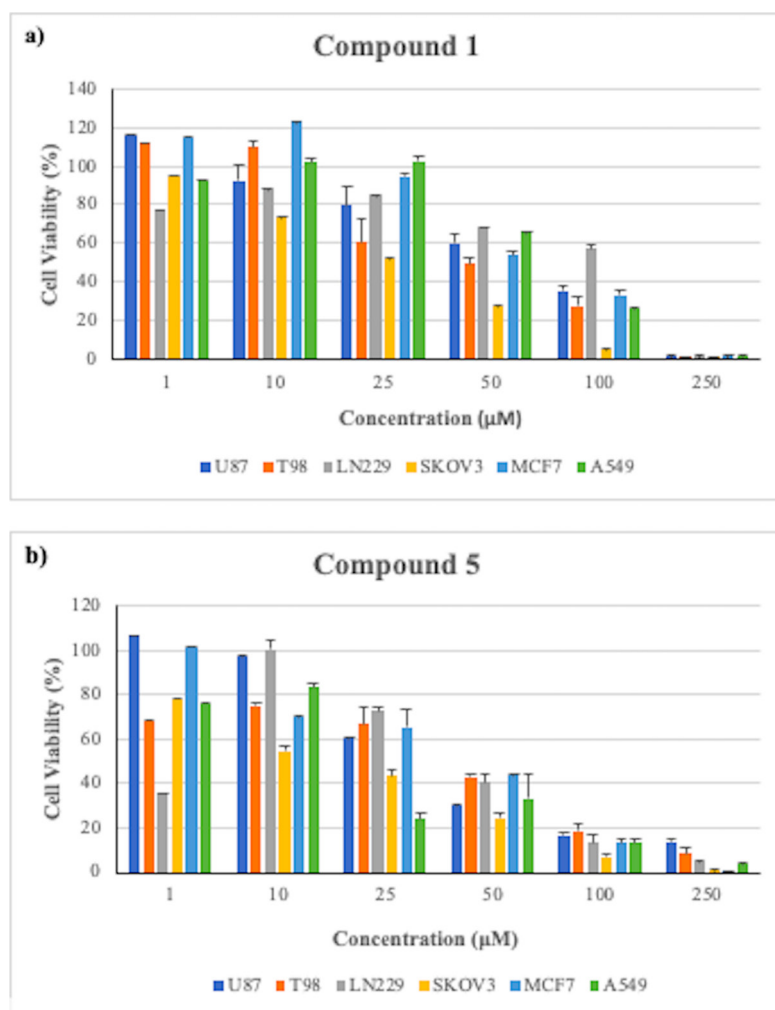


Figure 2. Synthesis of Compound 1-9.

Table 1. The IC₅₀ values of synthesized novel oxadiazole compounds, CAPE, and CA on U87, T98G, and LN229 cells.

IC ₅₀ (μM)			
Compound	U87	T98G	LN229
1	60.3	39.2	80.4
2	117.1	85.5	108.2
3	277.1	90.8	51
4	95.3	258.6	132.6
5	35.1	34.4	37.9
6-9	nd*	>250	>250
CA	nd*	51.5	56.6
CAPE	97.1	97.9	118.2

*nd: not detected

**Figure 3.** Cytotoxic activity of novel oxadiazole (a) compounds 1 and (b) 5 at 1–250 μM concentrations on different cancer cell lines at 48 h incubation. The error bars show SEM.

IC₅₀ values of compound **1** was determined as 60.3, 39.2, and 80.4 μM in U87, T98G, and LN229 cells, respectively. To clarify the effect of -CF₃ group on the inhibitory activity, the result of compound **3** was compared with compound **1**, it was concluded that this group did not increase the activity positively.

In addition, compound **5**, possessing 1,3,4-oxadiazole ring was found to have the highest inhibitory activity in comparison to the all other oxadiazoles and reference molecules CA and CAPE. The IC₅₀ values of compound **5** in U87, T98G, and LN229 cells were determined as 35.1, 34.4, and 37.9 μM , respectively (Table 1). To examine the effects of furyl and phenyl (R₃) rings on inhibitory activity, compounds **4** and **5** were prepared and compound **5** with furyl ring showed better inhibitory activity in GBM cell lines. Compounds **6-9** have no significant inhibitory activity on the GBM cell lines. When we compare the inhibitory activity of the compounds **4-5** with compounds **6-9**, it was clear that the dihydroxy group of the 1,3,4-oxadiazoles in the phenylpropanoid structure significantly increased the activity.

Cell viability analysis was performed in SKOV3 (ovarian cancer), MCF7 (breast cancer), and A549 (lung cancer) cells for compounds **1** and **5**, compound **5** showed higher cytotoxicity than references CA and CAPE in GBM cells lines. The IC₅₀ values are listed in Table 2.

In comparison to GBM cell lines, SKOV3, MCF7, and A549 cells showed higher sensitivity towards compounds **5** and **1**. The IC₅₀ values of compound **5** were determined as 14.2, 30.9, and 18.3 μM in SKOV3, MCF7, and A549 cells, respectively. Based on these results, compound **5** appears to be more active than both compound **1** and references CAPE and CA in these three different cancer cells.

In addition, cell viability assay was performed on healthy hMSC in the range of 1–50 μM values to examine the effects of compound **5** and **1** and references CAPE and CA. When the hMSC cells incubated with compounds **5**, **1** and references CAPE, CA with in the 50 μM (highest concentration) values for 48 h, cell viability was found 94.59%, 57.62% and 16.89%, 19.22%, respectively (Figure 4).

Table 2. The IC₅₀ values of synthesized novel oxadiazole compounds, CAPE, and CA on SKOV3, MCF7, and A549 cells.

IC ₅₀ (μM)			
Compound	SKOV3	MCF7	A549
1	21.1	70.9	62
5	14.2	30.9	18.3
CA	38.4	46.1	74.9
CAPE	35.5	61.2	191.3

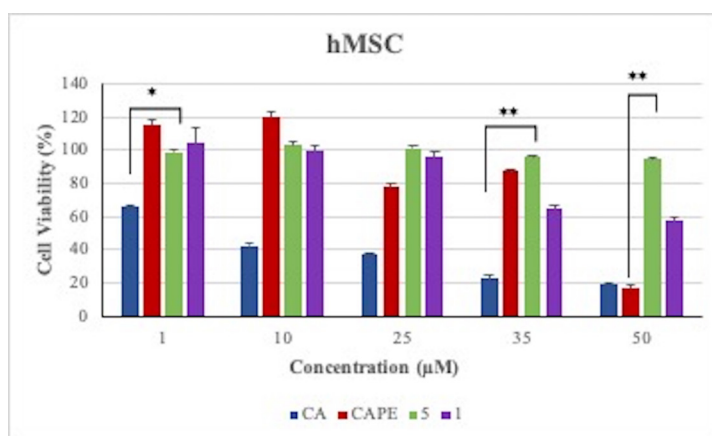


Figure 4. Cell viability results of compounds **1**, **5**, CAPE, and CA at 1–50 μM concentrations on hMSC cells. The error bars show SEM, * $p < 0.05$, and ** $p < 0.01$ considered significant (calculated using paired t-test).

4. Conclusion

Novel oxadiazole derivatives were synthesized and evaluated for their anticancer activities in different cancer cells. The most promising results were obtained with compound **1** and **5**, carrying 1,2,4-oxadiazole and 1,3,4-oxadiazole moieties, respectively. Compound **5** showed similar activity ($35 \pm 2 \mu\text{M}$) against all GBM cell lines. In addition, compounds **1** and **5** significantly inhibit cell proliferation at low concentrations in different cancer cell lines, such as ovarian, breast, and lung. Moreover, the active compounds did not show any toxicity towards the selected nonmalignant cell lines. The results indicate that it is possible to synthesize various derivatives which could be used in further studies to investigate different pathways in cancer.

Acknowledgement

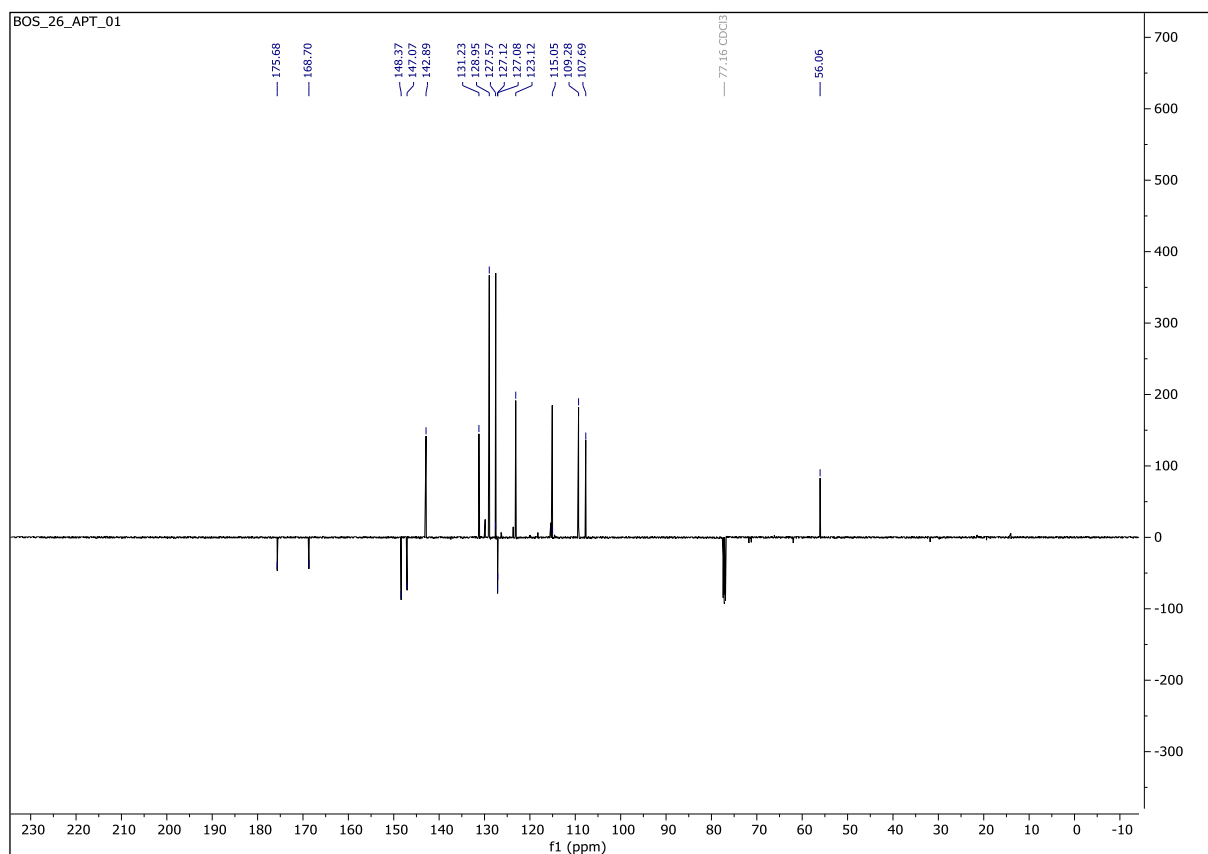
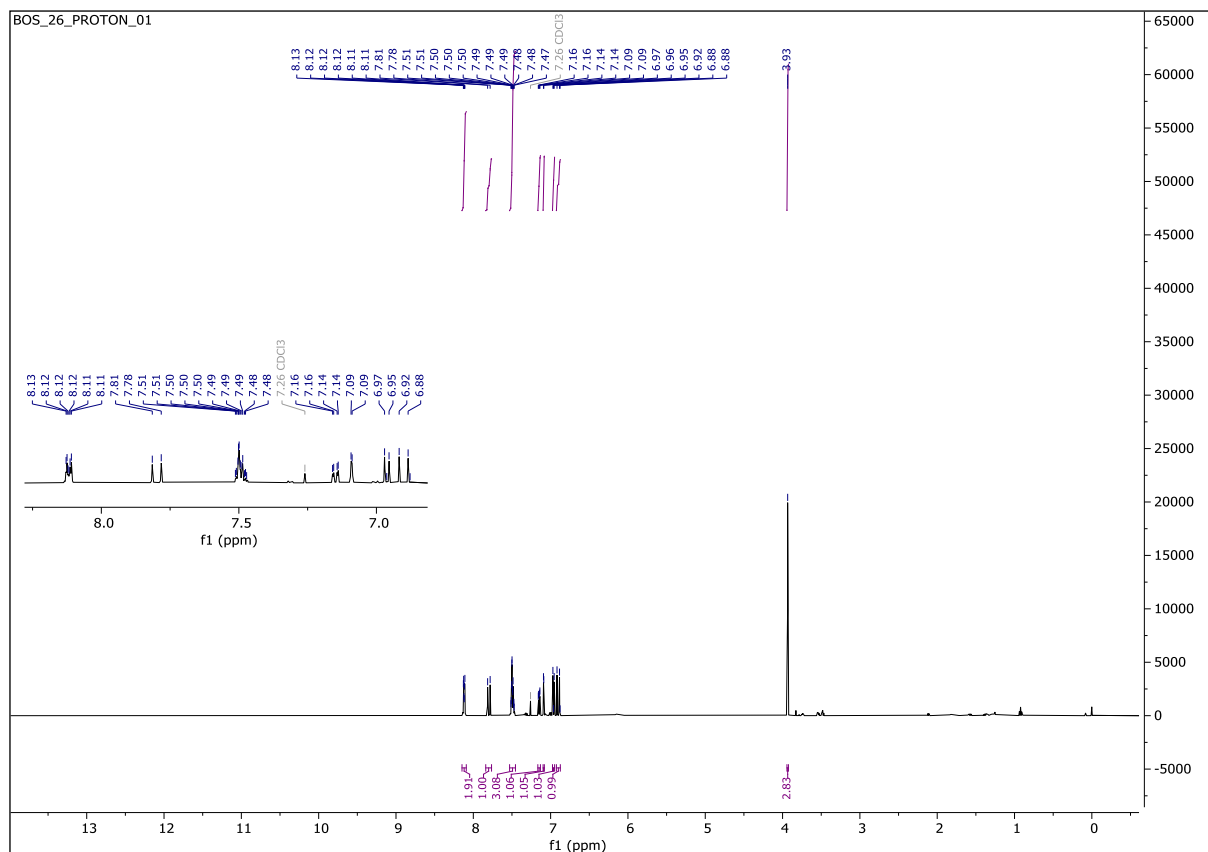
We thank the Scientific and Technological Research Council of Turkey (TÜBİTAK) for its financial support (project no:119Z116).

References

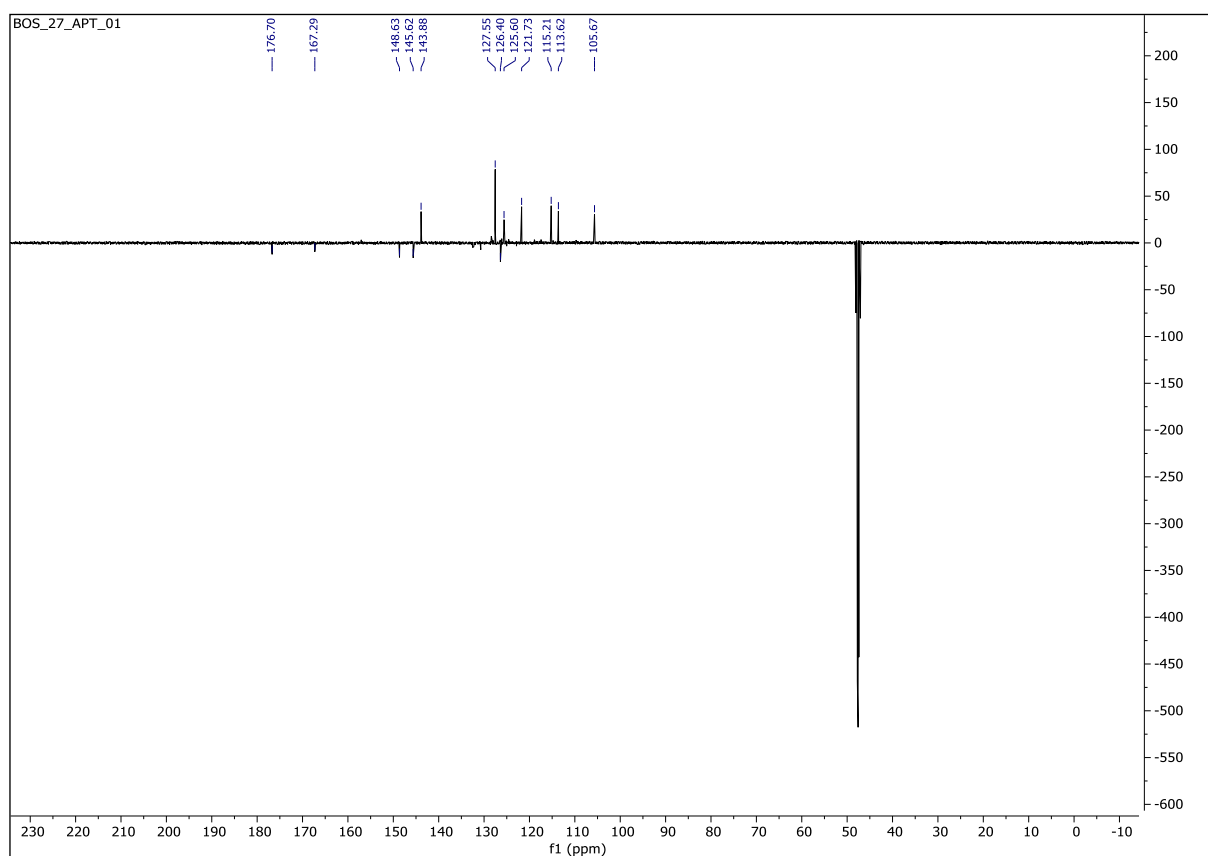
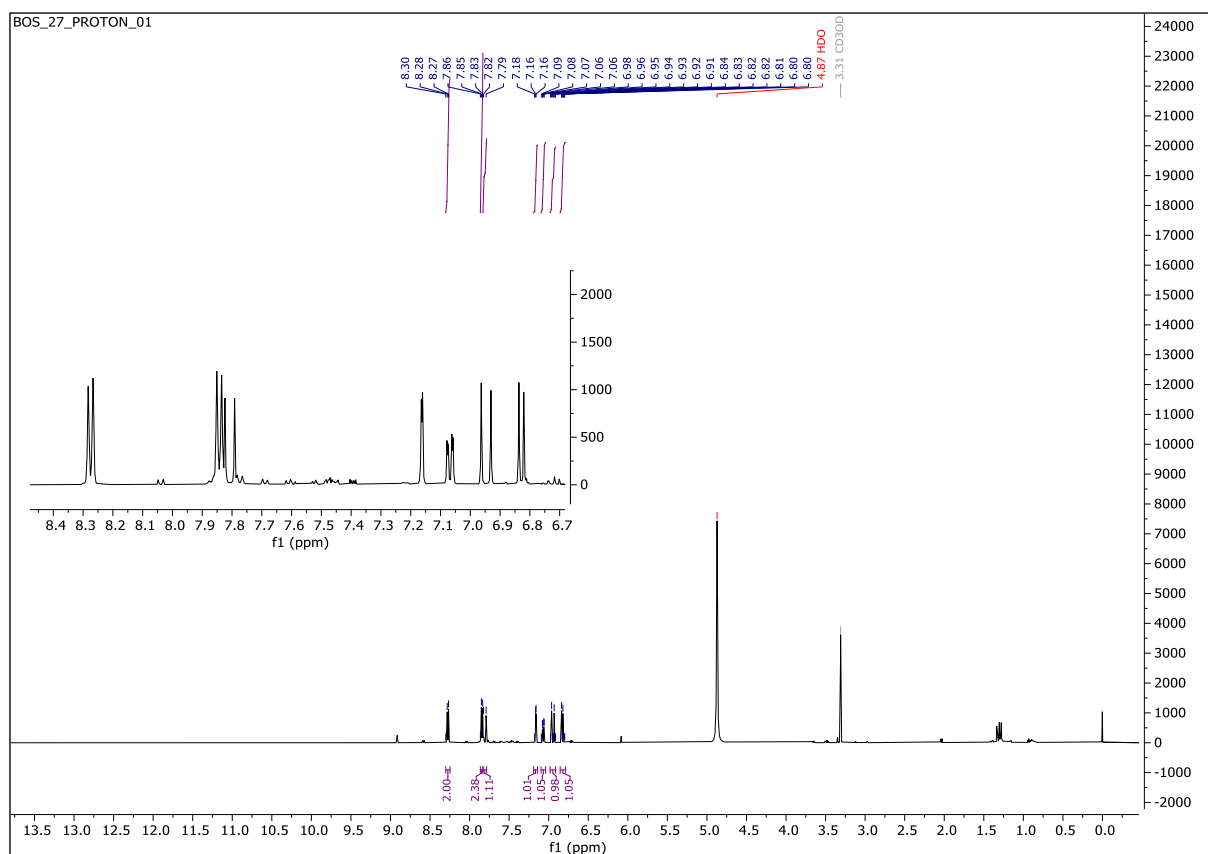
1. Szoka L, Palka J. Capsaicin up-regulates pro-apoptotic activity of thiazolidinediones in glioblastoma cell line. *Biomedicine and Pharmacotherapy* 2020; 132: 110741. doi: 10.1016/j.biopha.2020.110741
2. Hönikl LS, Lämmer F, Gempt J, Meyer B, Schlegel J et al. High expression of estrogen receptor alpha and aromatase in glial tumor cells is associated with gender-independent survival benefits in glioblastoma patients. *Journal of Neuro-Oncology* 2020; 147: 567–75. doi: 10.1007/s11060-020-03467-y
3. Papadopoulou F, Isihou R, Alexiou GA, Tsaliotis T, Vartholomatos E et al. Haloperidol induced cell cycle arrest and apoptosis in glioblastoma cells. *Biomedicines* 2020; 8: 1–12.
4. Oh HC, Shim JK, Park J, Lee JH, Choi RJ et al. Combined effects of niclosamide and temozolomide against human glioblastoma tumorspheres. *Journal of Cancer Research and Clinical Oncology* 2020; 146: 2817–28. doi: 10.1007/s00432-020-03330-7
5. Hu S, Kang H, Baek Y, El Fakhri G, Kuang A et al. Real-Time Imaging of Brain Tumor for Image-Guided Surgery. *Advanced Healthcare Materials* 2018; 7: 1–15.
6. Malhotra M, Sekar TV, Ananta JS, Devulapally R, Afjei R et al. Targeted nanoparticle delivery of therapeutic antisense microRNAs presensitizes glioblastoma cells to lower effective doses of temozolomide in vitro and in a mouse model. *Oncotarget* 2018; 9: 21478–94.
7. Cuperlovic-Culf M, Touaibia M, St-Coeur PD, Poitras J, Morin P et al. Metabolic effects of known and novel HDAC and SIRT inhibitors in glioblastomas independently or combined with temozolomide. *Metabolites* 2014; 4: 807–30.
8. Perazzoli G, Prados J, Ortiz R, Caba O, Cabeza L et al. Temozolomide resistance in glioblastoma cell lines: Implication of MGMT, MMR, P-glycoprotein and CD133 expression. *PLoS ONE* 2015; 10: 1–23.
9. Feng J, Yan PF, Zhao HY, Zhang FC, Zhao WH et al. Inhibitor of nicotinamide phosphoribosyltransferase sensitizes glioblastoma cells to temozolomide via activating ROS/JNK signaling pathway. *BioMed Research International* 2016; 2016: 1450843.
10. Chen SH, Chao CN, Chen SY, Lin HP, Huang HY et al. Flunarizine, a drug approved for treating migraine and vertigo, exhibits cytotoxicity in GBM cells. *European Journal of Pharmacology* 2020; 892: 173756. doi: 10.1016/j.ejphar.2020.173756
11. Mirzaei S, Gholami MH, Zabolian A, Saleki H, Farahani MV et al. Caffeic acid and its derivatives as potential modulators of oncogenic molecular pathways: New hope in the fight against cancer. *Pharmacological Research* 2021; 171: 105759. doi: 10.1016/j.phrs.2021.105759
12. Rajendra Prasad N, Karthikeyan A, Karthikeyan S, Venkata Reddy B. Inhibitory effect of caffeic acid on cancer cell proliferation by oxidative mechanism in human HT-1080 fibrosarcoma cell line. *Molecular and Cellular Biochemistry* 2011; 349: 11–9.
13. Eroğlu C, Seçme M, Bağcı G, Dodurga Y. Assessment of the anticancer mechanism of ferulic acid via cell cycle and apoptotic pathways in human prostate cancer cell lines. *Tumor Biology* 2015; 36: 9437–46.
14. Stähli A, Maheen CU, Strauss FJ, Eick S, Sculean A et al. Caffeic acid phenethyl ester protects against oxidative stress and dampens inflammation via heme oxygenase 1. *International Journal of Oral Science* 2019; 11: 1–8. doi: 10.1038/s41368-018-0039-5
15. Matsunaga T, Tsuchimura S, Azuma N, Endo S, Ichihara K et al. Caffeic acid phenethyl ester potentiates gastric cancer cell sensitivity to doxorubicin and cisplatin by decreasing proteasome function. *Anti-Cancer Drugs* 2019; 30: 251–9.
16. Liang Y, Feng G, Wu L, Zhong S, Gao X et al. Caffeic acid phenethyl ester suppressed growth and metastasis of nasopharyngeal carcinoma cells by inactivating the NF- κ B pathway. *Drug Design, Development and Therapy* 2019; 13: 1335–45.
17. Zhang X, Lin D, Jiang R, Li H, Wan J et al. Ferulic acid exerts antitumor activity and inhibits metastasis in breast cancer cells by regulating epithelial to mesenchymal transition. *Oncology Reports* 2016; 36: 271–8.

18. Serafim TL, Carvalho FS, Marques MPM, Calheiros R, Silva T et al. Lipophilic caffeic and ferulic acid derivatives presenting cytotoxicity against human breast cancer cells. *Chemical Research in Toxicology* 2011; 24: 763–74.
19. Nagane M, Yamashita T, Vörös P, Kálai T, Hideg K et al. Synthesis and evaluation of paramagnetic caffeic acid phenethyl ester (CAPE) analogs. *Monatshfte fur Chemie* 2019; 150: 1513–22. doi: 10.1007/s00706-019-02458-8
20. Boström J, Hogner A, Llinàs A, Wellner E, Plowright AT. Oxadiazoles in medicinal chemistry. *Journal of Medicinal Chemistry* 2012; 55: 1817–30.
21. Ali MA, Shaharyar M. Oxadiazole mannich bases: Synthesis and antimycobacterial activity. *Bioorganic and Medicinal Chemistry Letters* 2007; 17: 3314–6.
22. Zampieri D, Mamolo MG, Laurini E, Fermeglia M, Posocco P et al. Antimycobacterial activity of new 3,5-disubstituted 1,3,4-oxadiazol-2(3H)-one derivatives. *Molecular modeling investigations. Bioorganic & Medicinal Chemistry* 2009; 17: 4693–707.
23. Husain A, Ajmal M. Synthesis of novel 1,3,4-oxadiazole derivatives and their biological properties. *Acta Pharmaceutica* 2009; 59: 223–33.
24. Singh P, Sharma P, Sharma J, Upadhyay A, Kumar N. Synthesis and evaluation of substituted diphenyl-1,3,4-oxadiazole derivatives for central nervous system depressant activity. *Organic and Medicinal Chemistry Letters* 2012; 2: 8.
25. Song Y, Connor DT, Sercel AD, Sorenson RJ, Doubleday R et al. Synthesis, structure-activity relationships, and in vivo evaluations of substituted di-tert-butylphenols as a novel class of potent, selective, and orally active cyclooxygenase-2 inhibitors. 2. 1,3,4- and 1,2,4-thiadiazole series. *Journal of Medicinal Chemistry* 1999; 42: 1161–9.
26. Bajaj S, Roy PP, Singh J. Synthesis, thymidine phosphorylase inhibitory and computational study of novel 1,3,4-oxadiazole-2-thione derivatives as potential anticancer agents. *Computational Biology and Chemistry* 2018; 76: 151–60.
27. Sucu BO, Koc EB, Savlug Ipek O, Mirat A, Almas F et al. Design and synthesis of novel caffeic acid phenethyl ester (CAPE) derivatives and their biological activity studies in glioblastoma multiforme (GBM) cancer cell lines. *Journal of Molecular Graphics and Modelling* 2022; 113: 108160. doi: 10.1016/j.jm gm.2022.108160
28. Tripathi A, Choubey PK, Sharma P, Seth A, Saraf P et al. Design, synthesis, and biological evaluation of ferulic acid based 1,3,4-oxadiazole hybrids as multifunctional therapeutics for the treatment of Alzheimer's disease. *Bioorganic Chemistry* 2020; 95: 103506. doi: 10.1016/j.bioorg.2019.103506

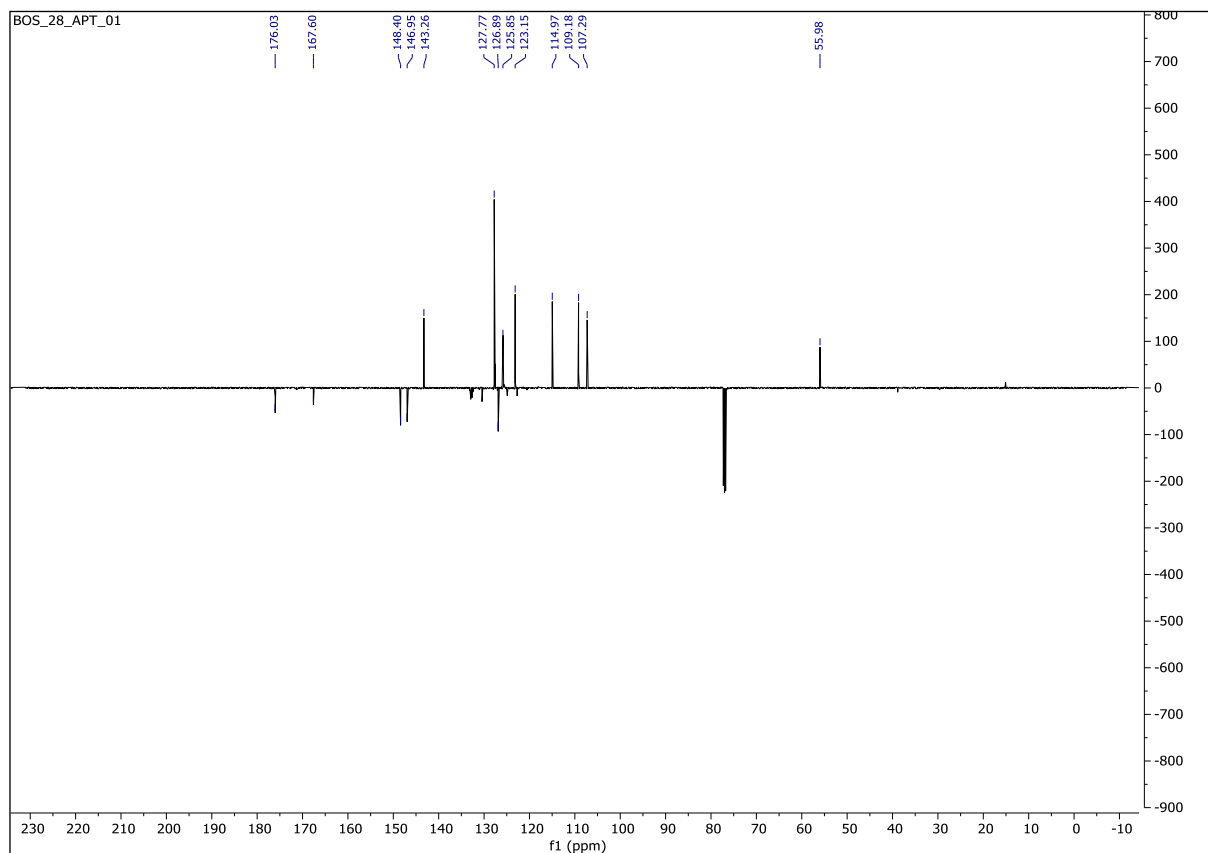
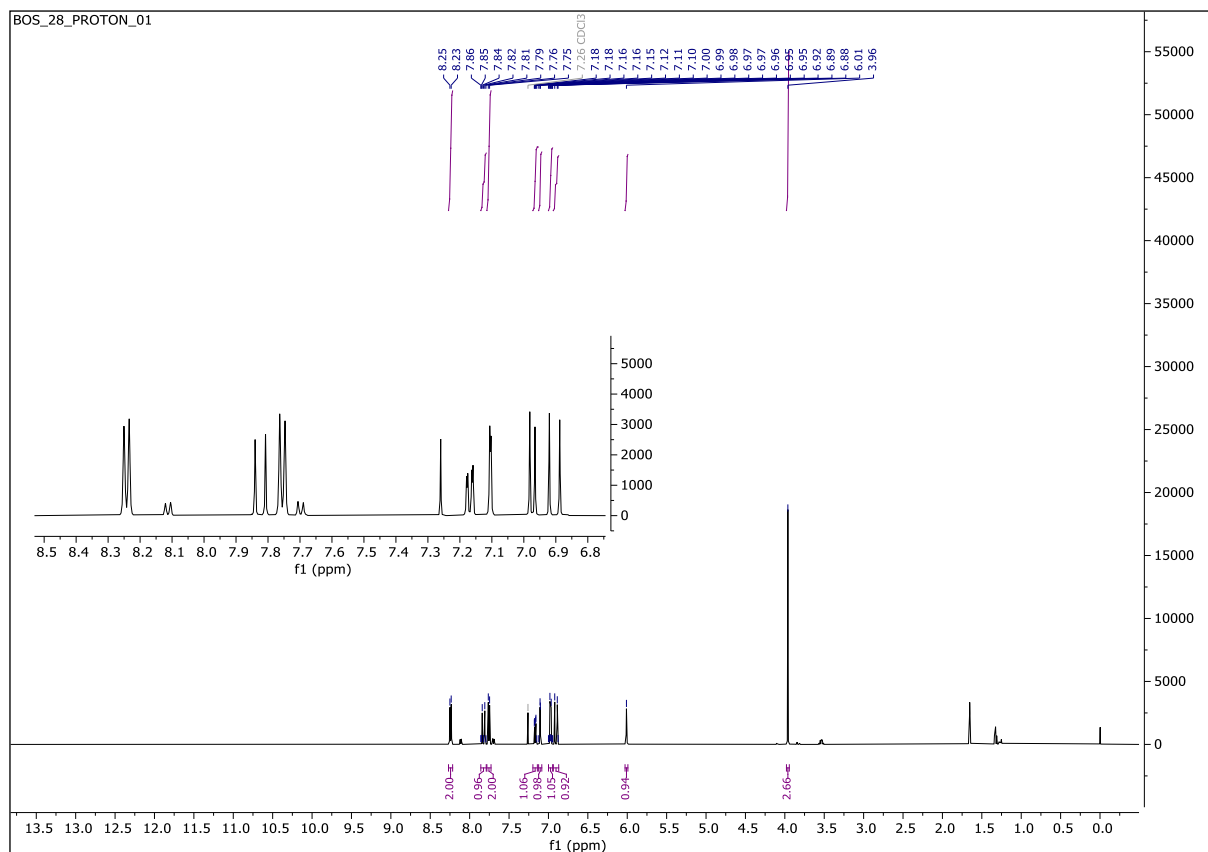
Compound 1



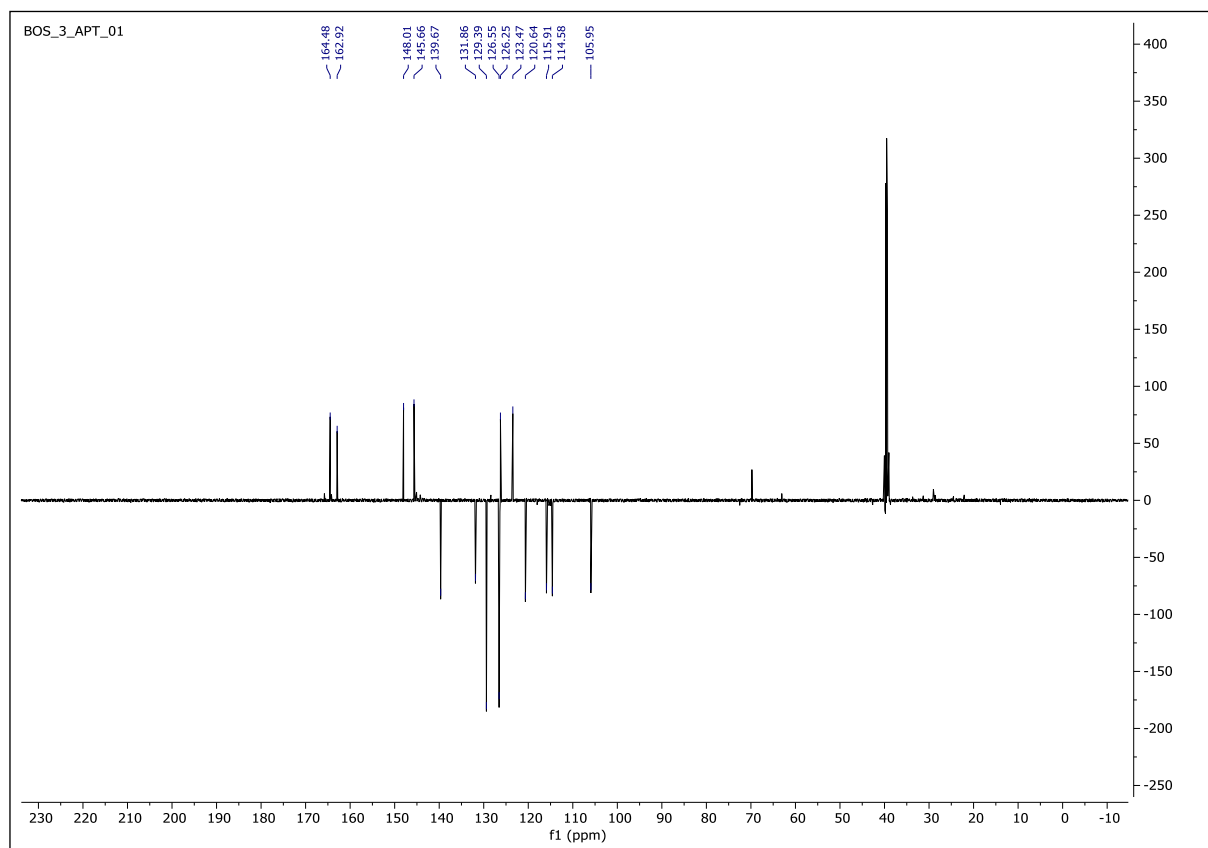
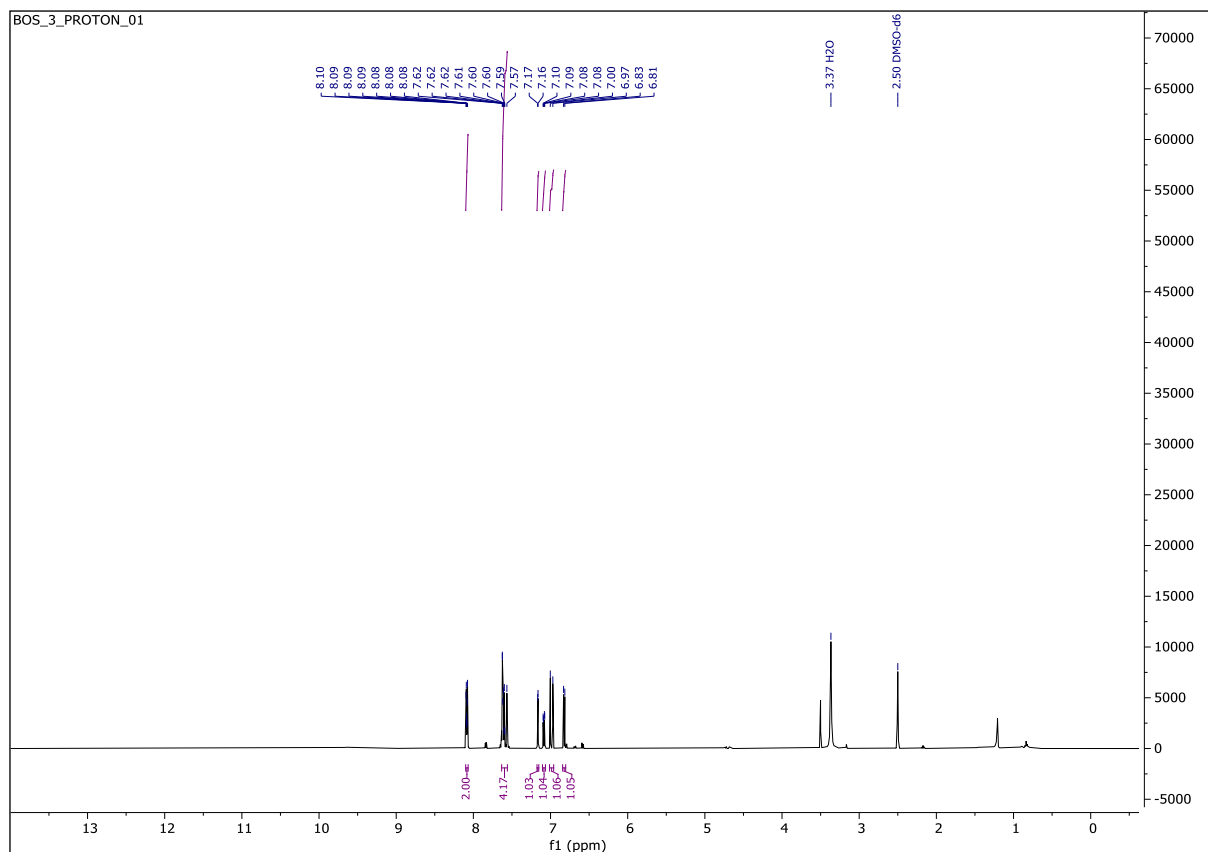
Compound 2



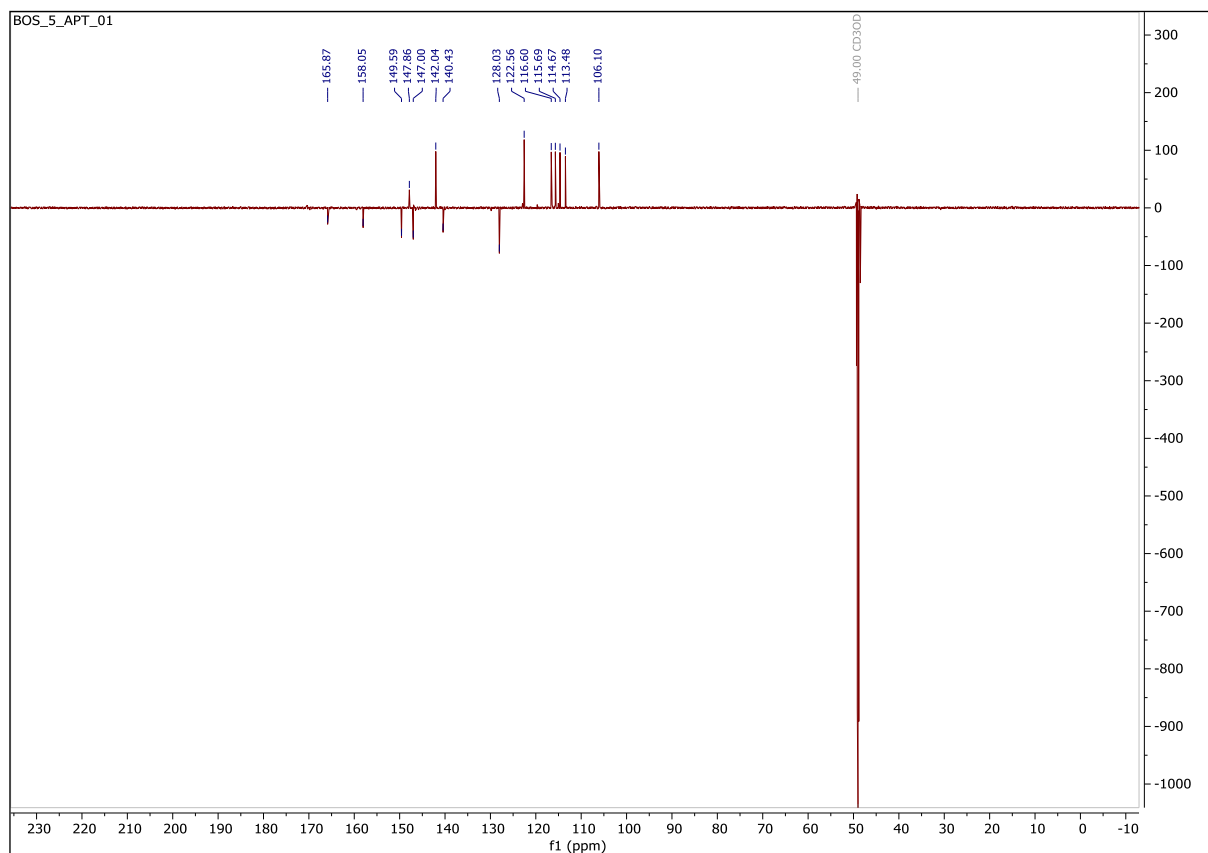
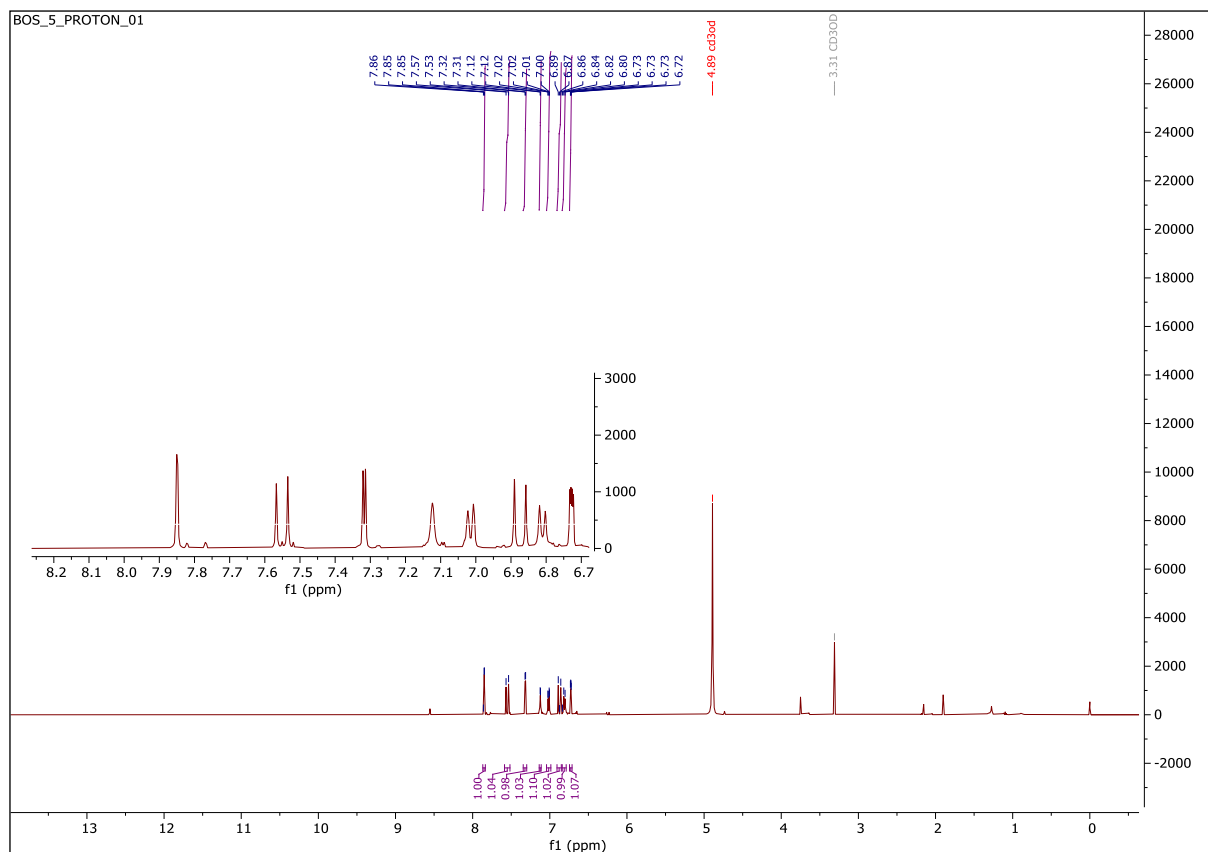
Compound 3



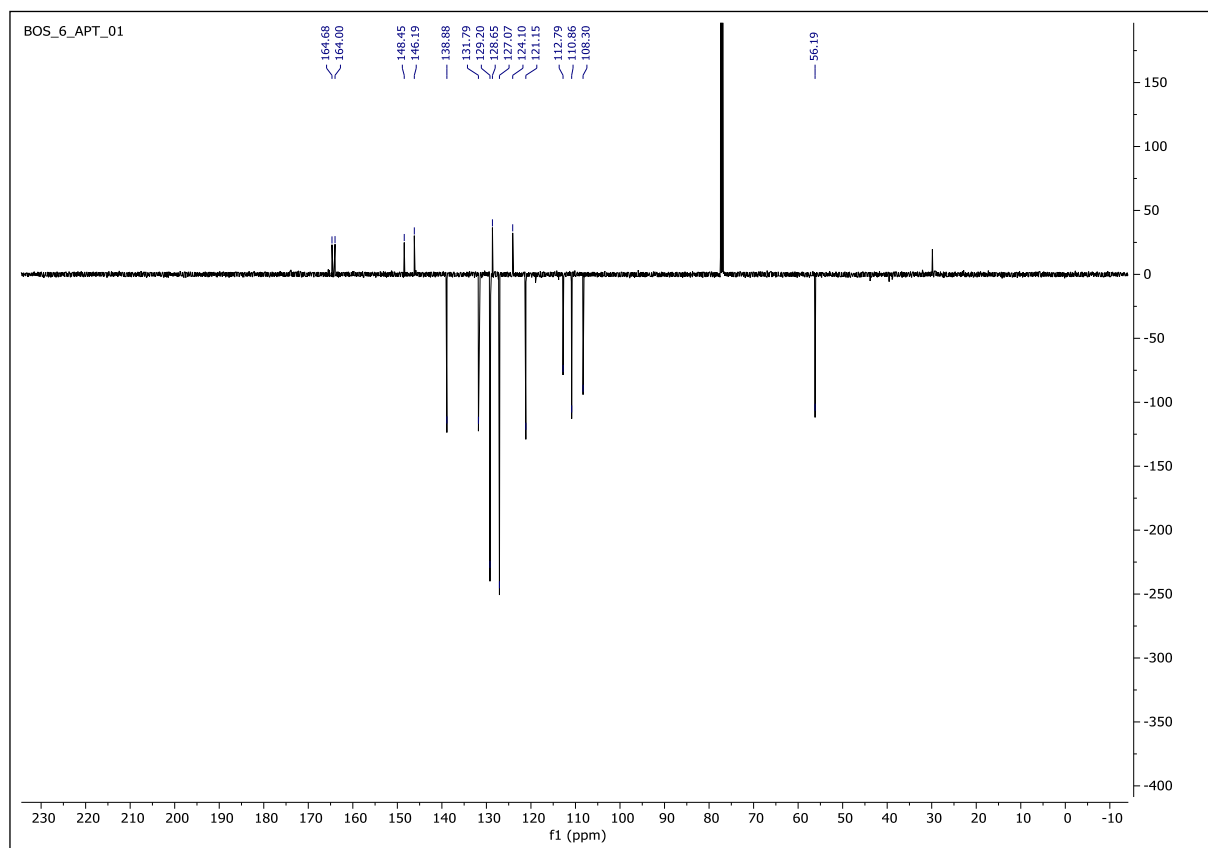
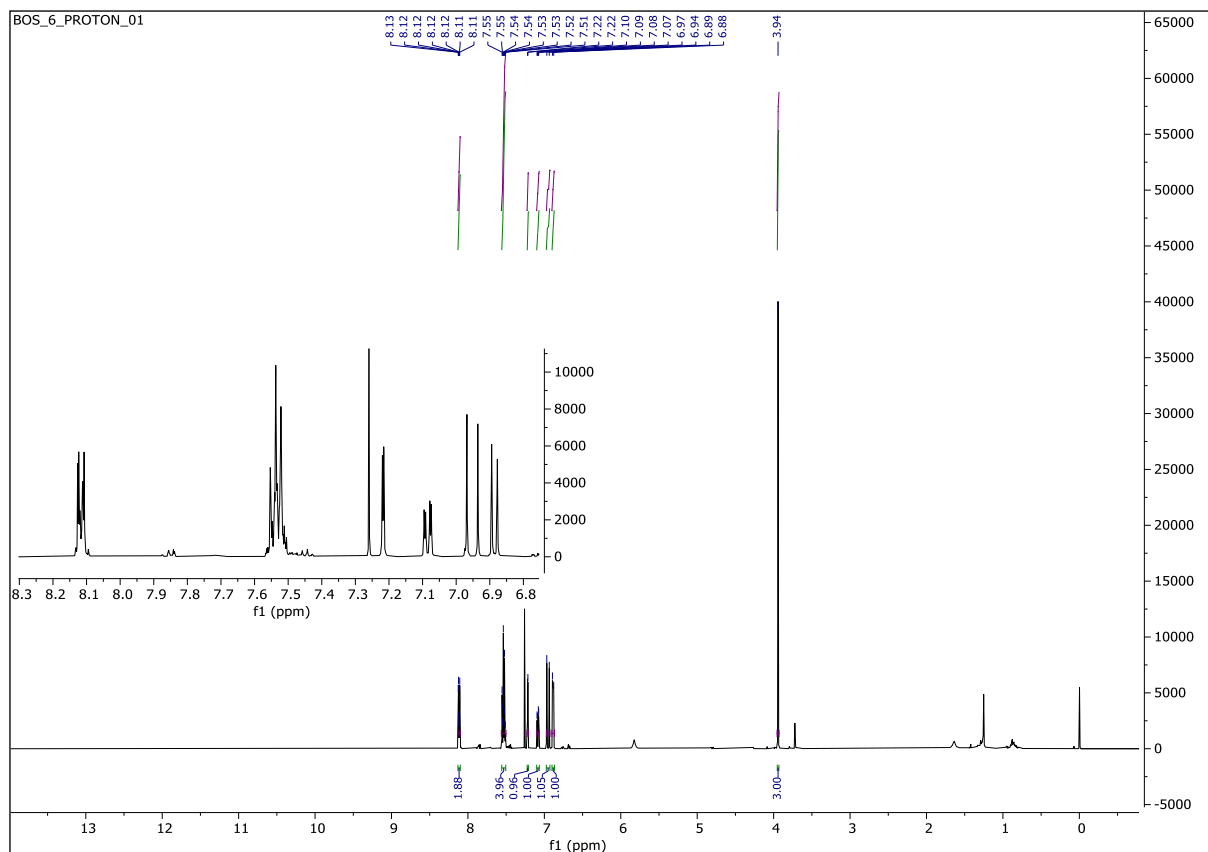
Compound 4



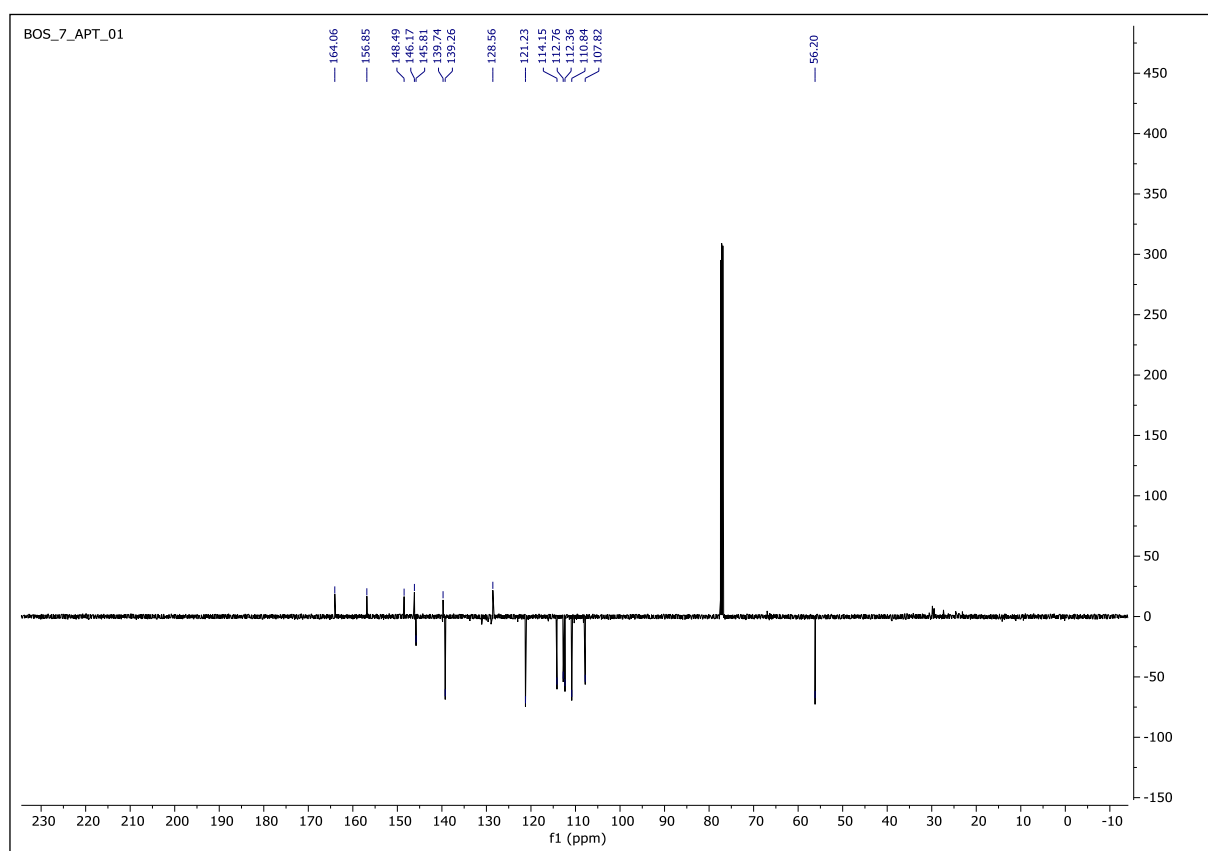
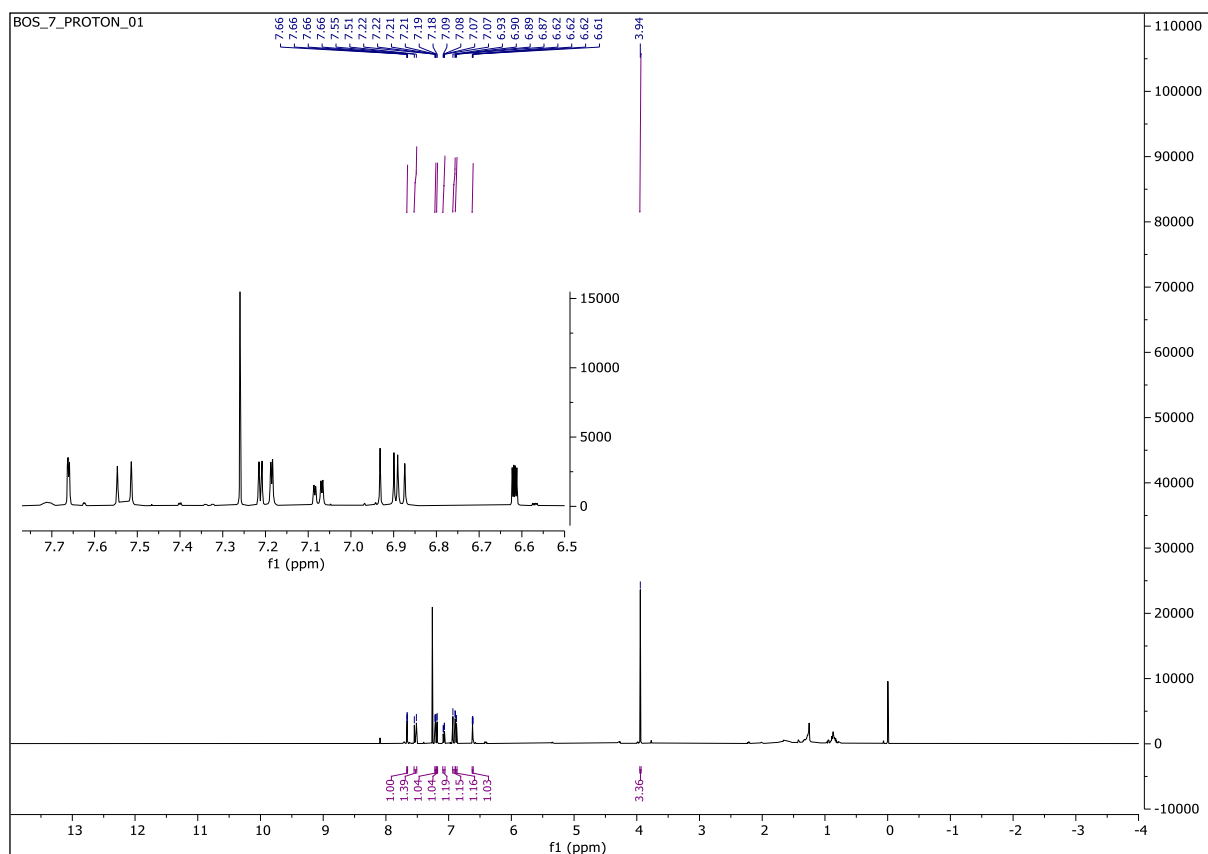
Compound 5



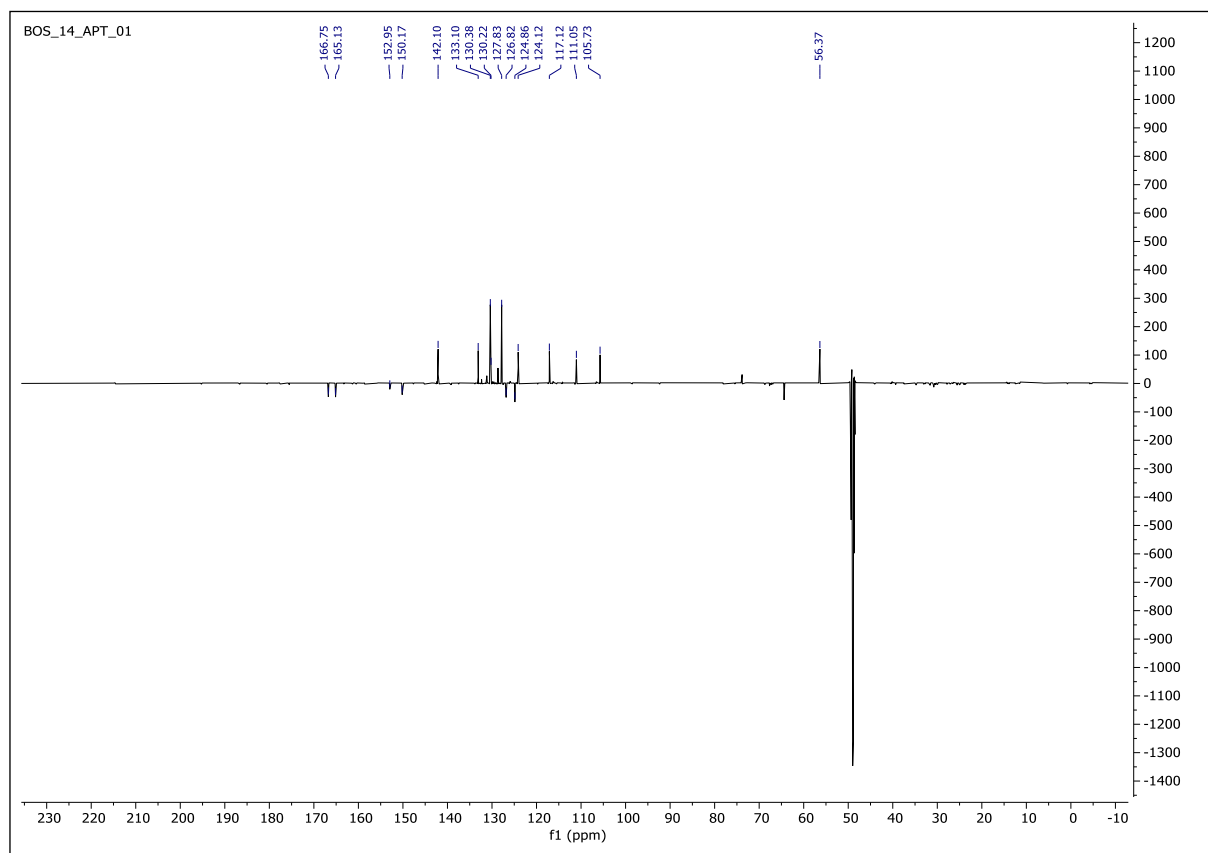
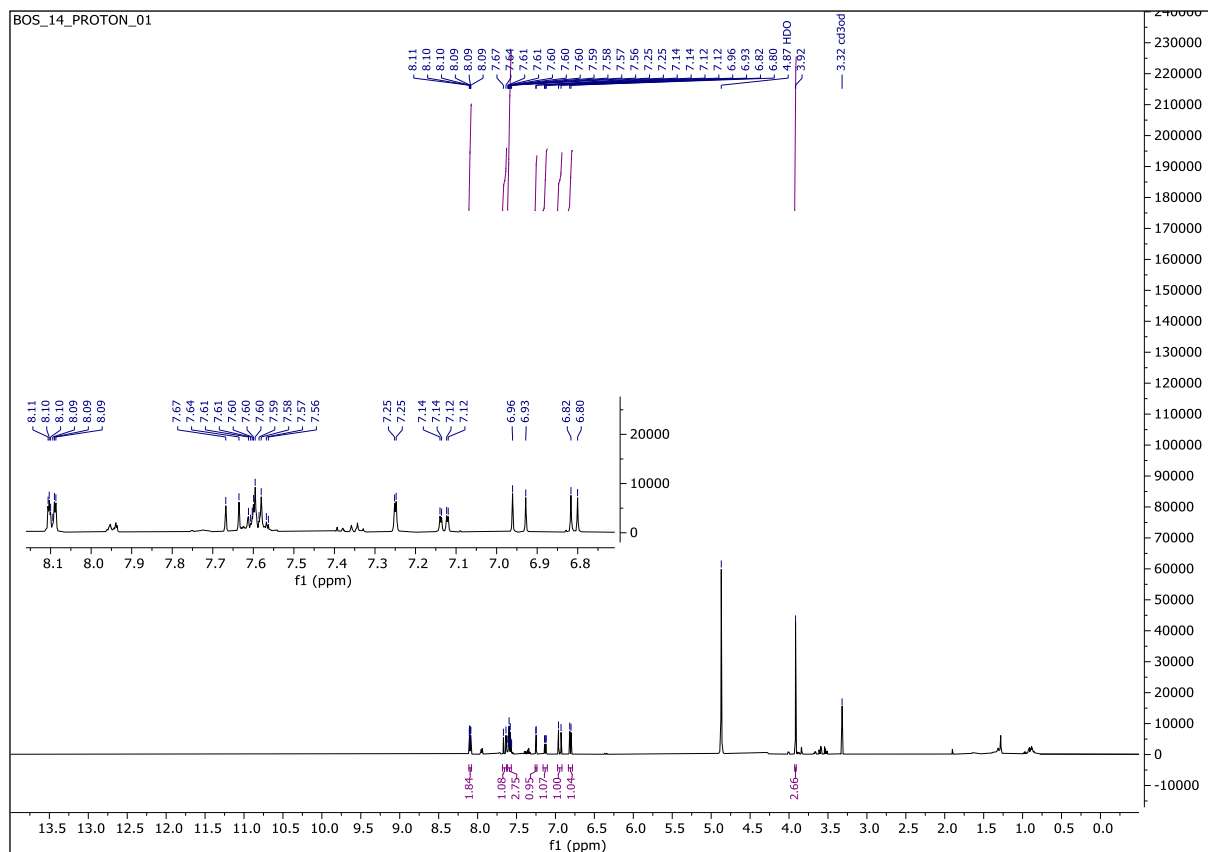
Compound 6



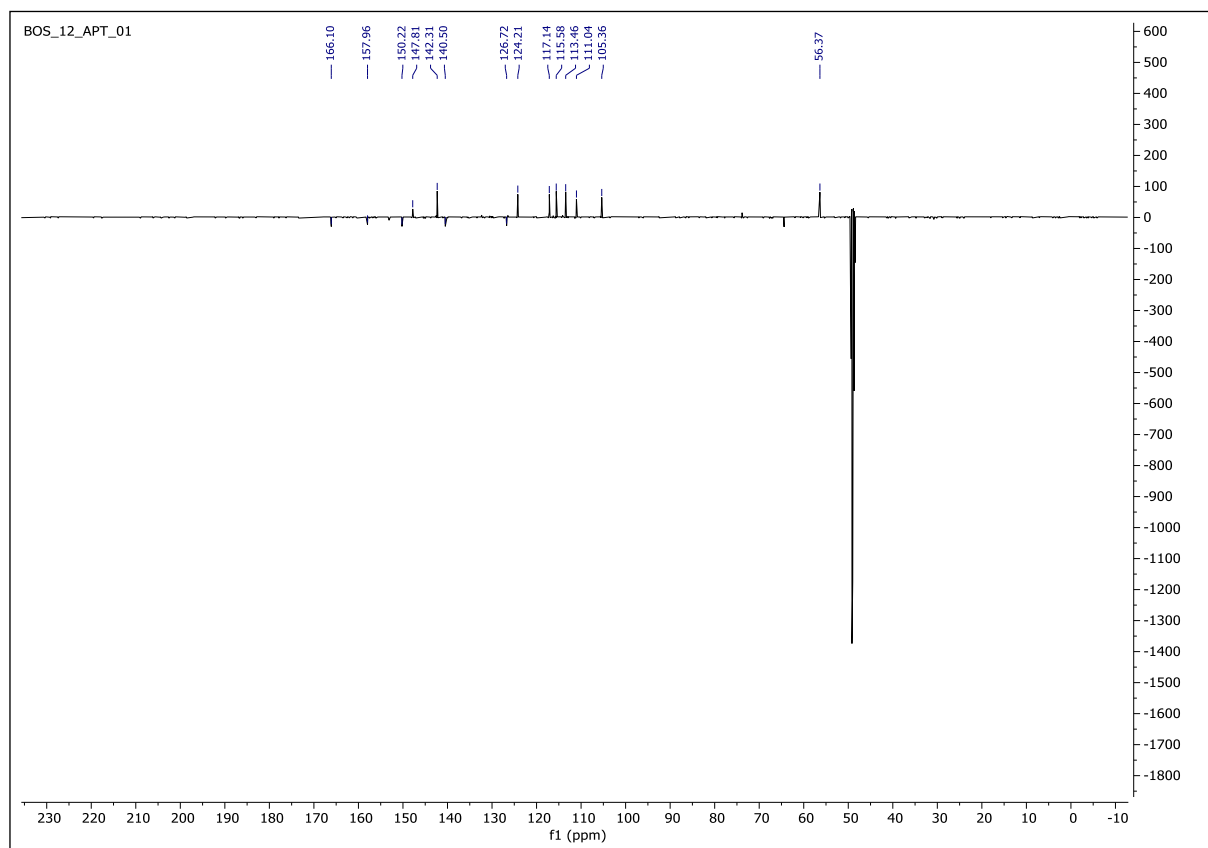
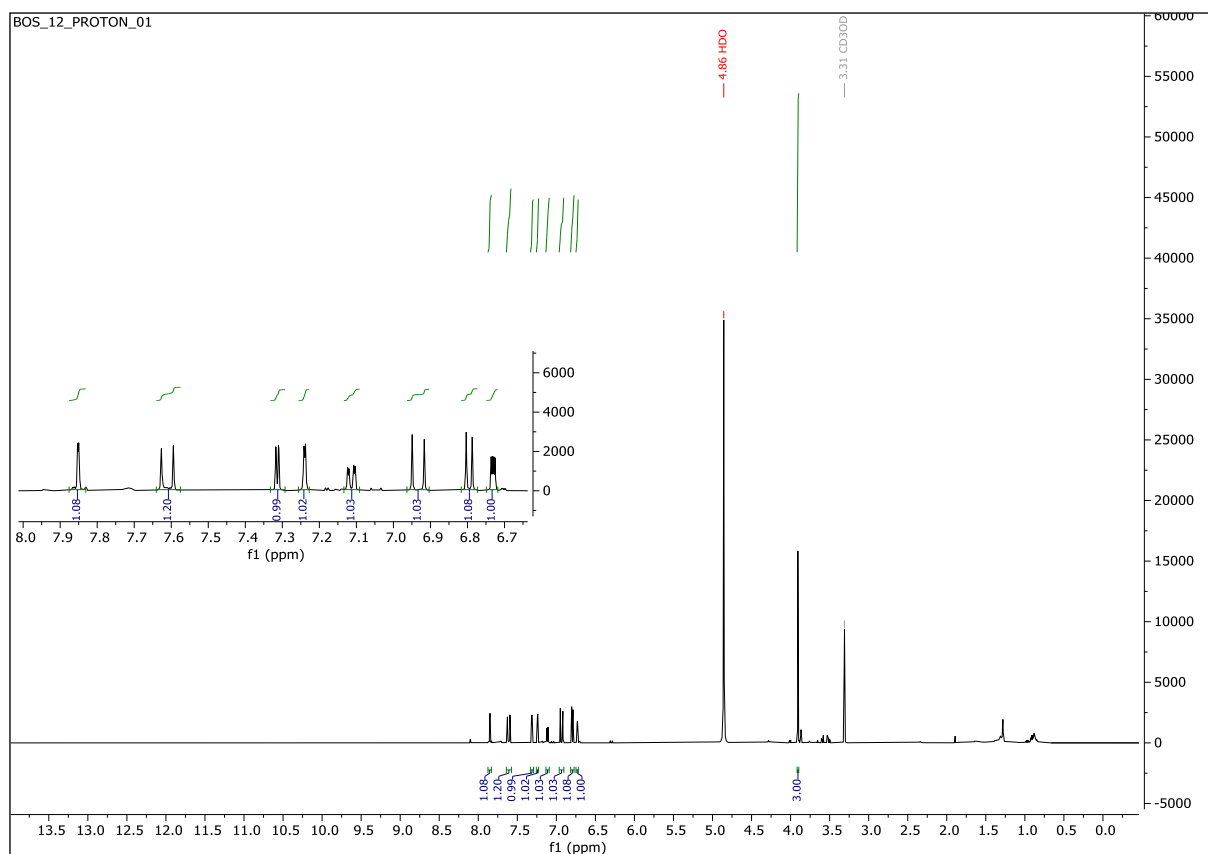
Compound 7



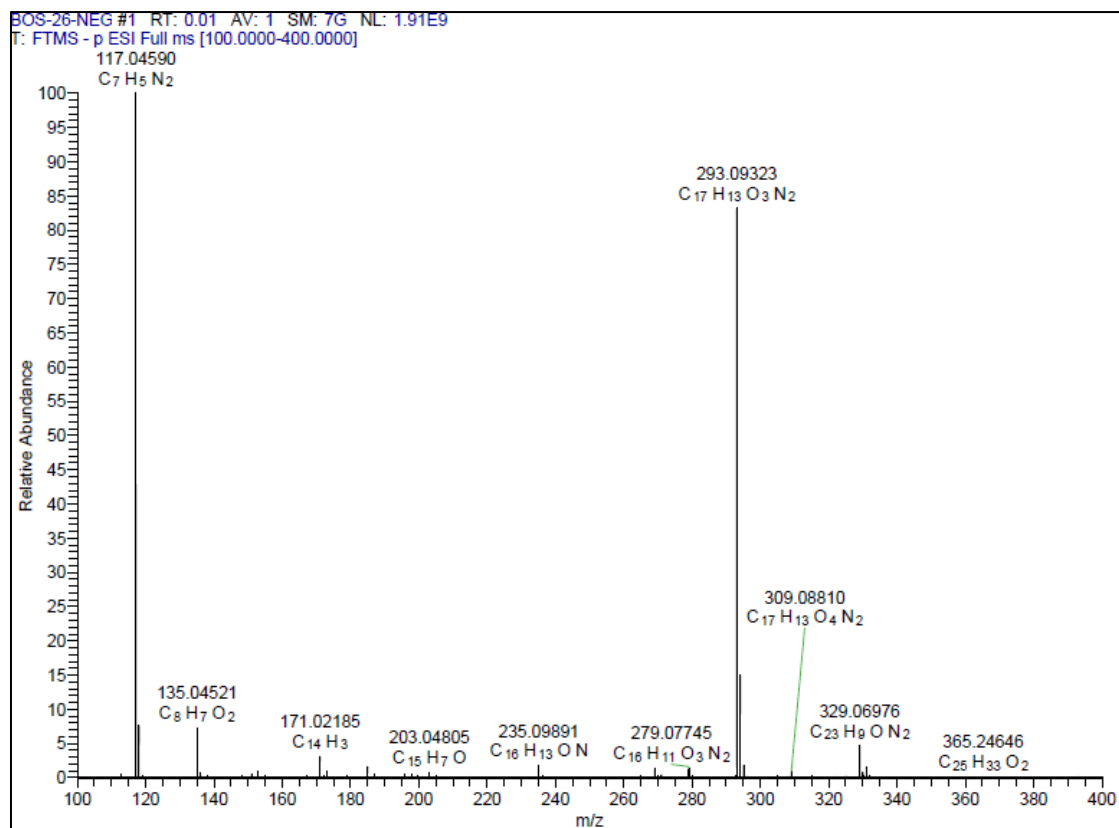
Compound 8



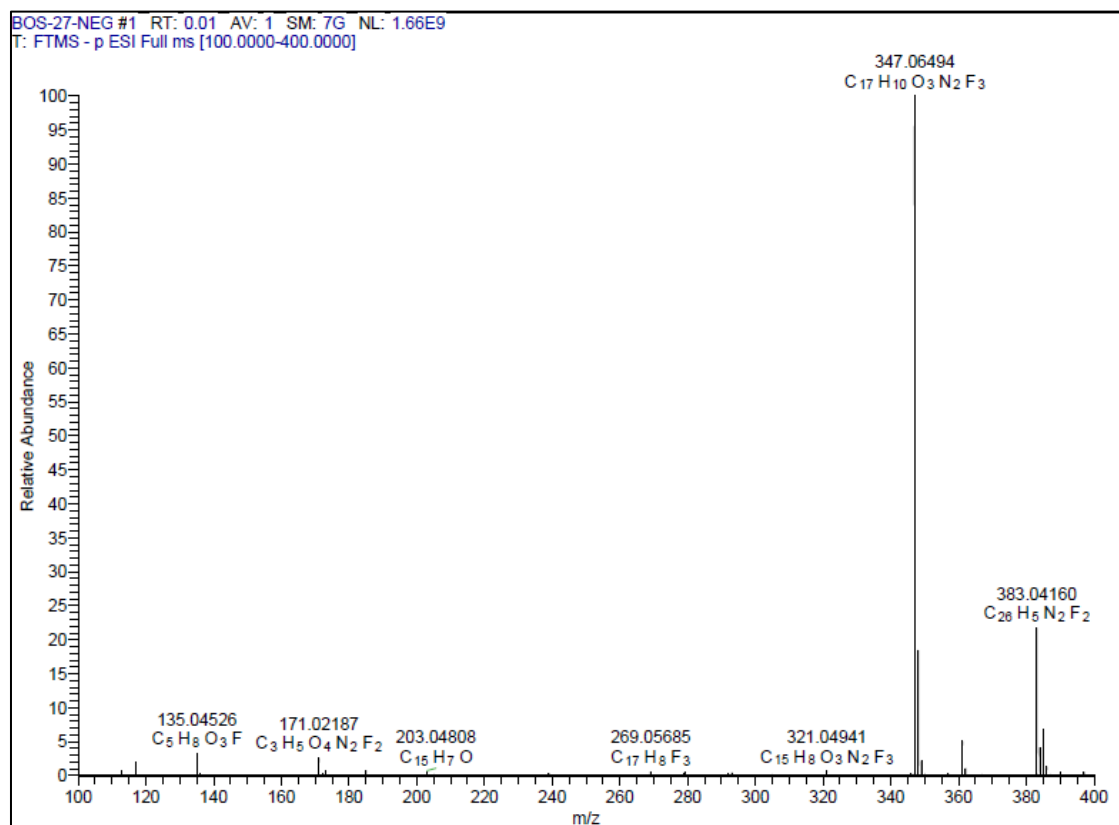
Compound 9



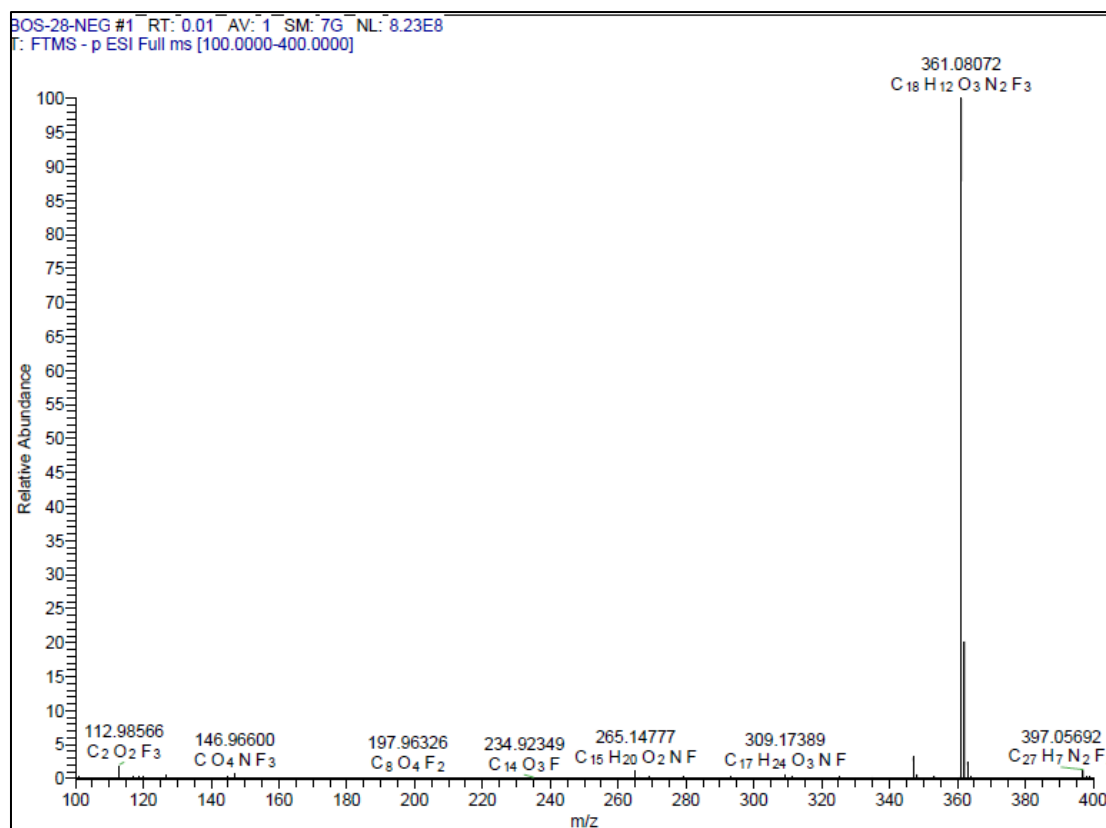
Compound 1



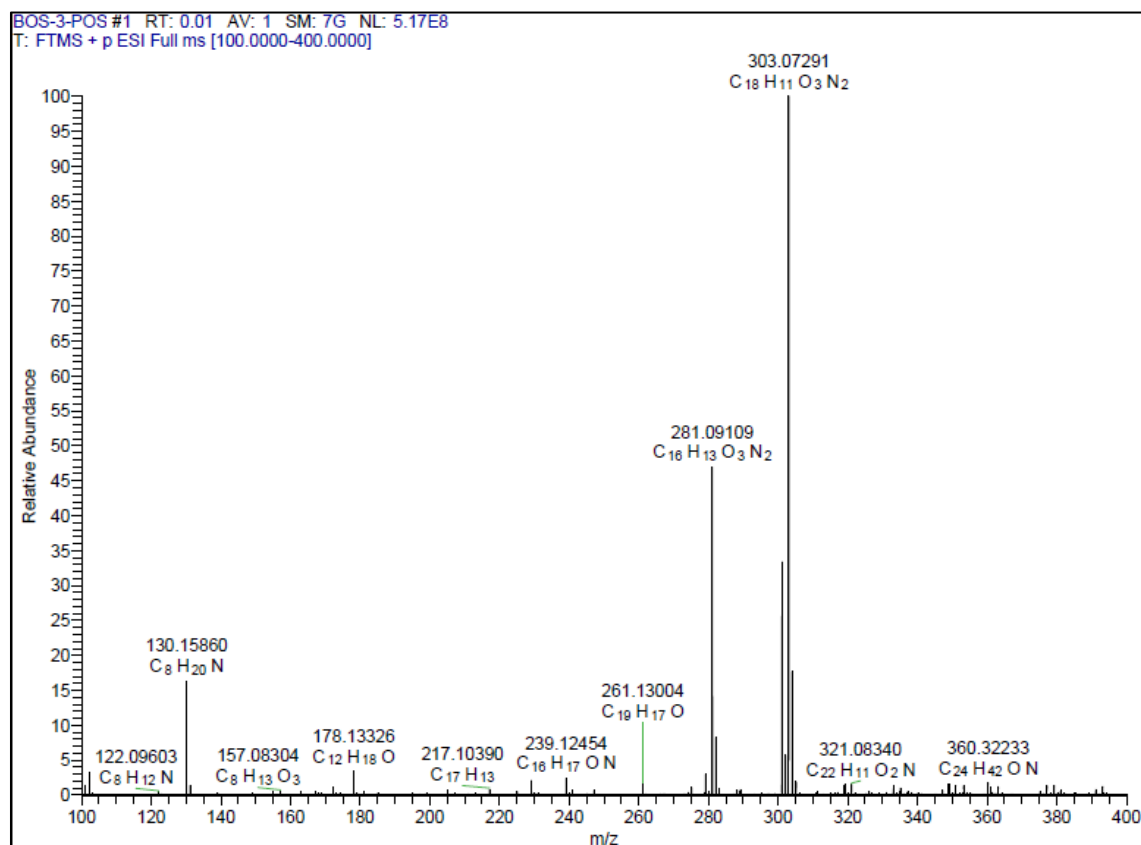
Compound 2



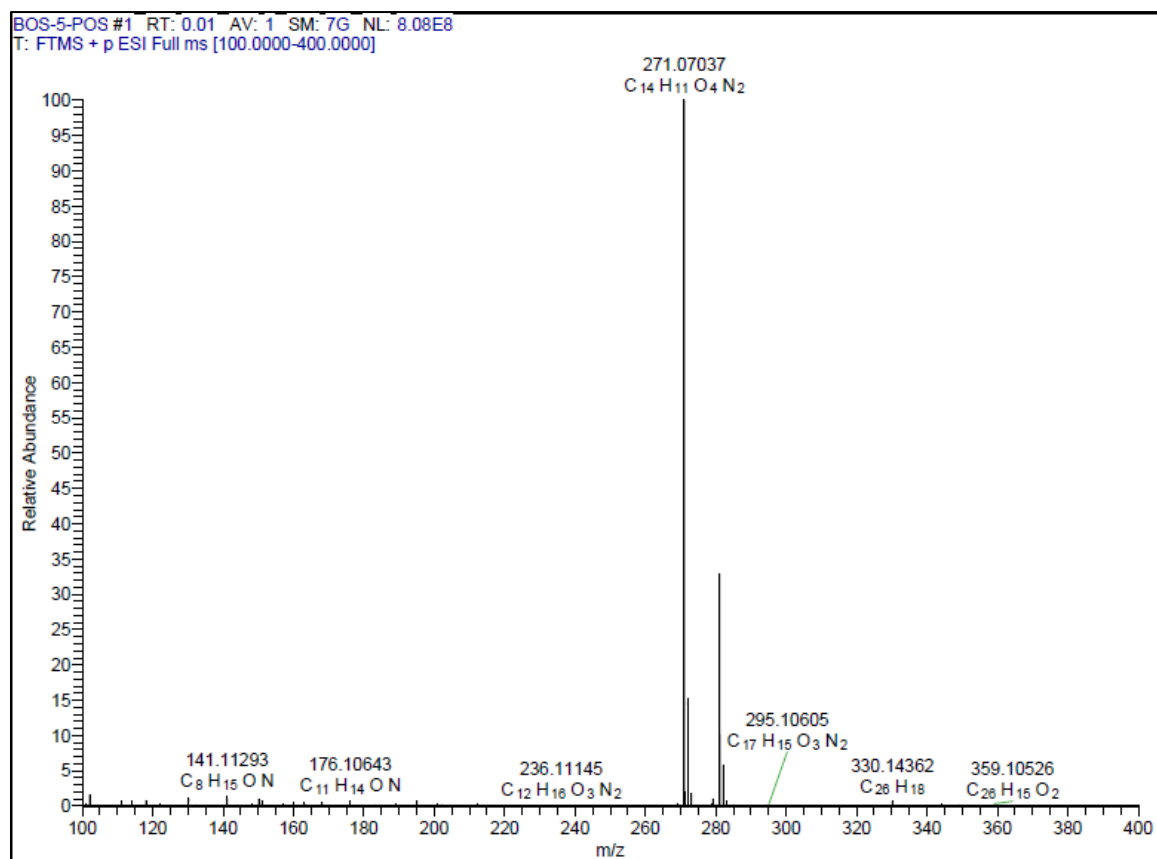
Compound 3



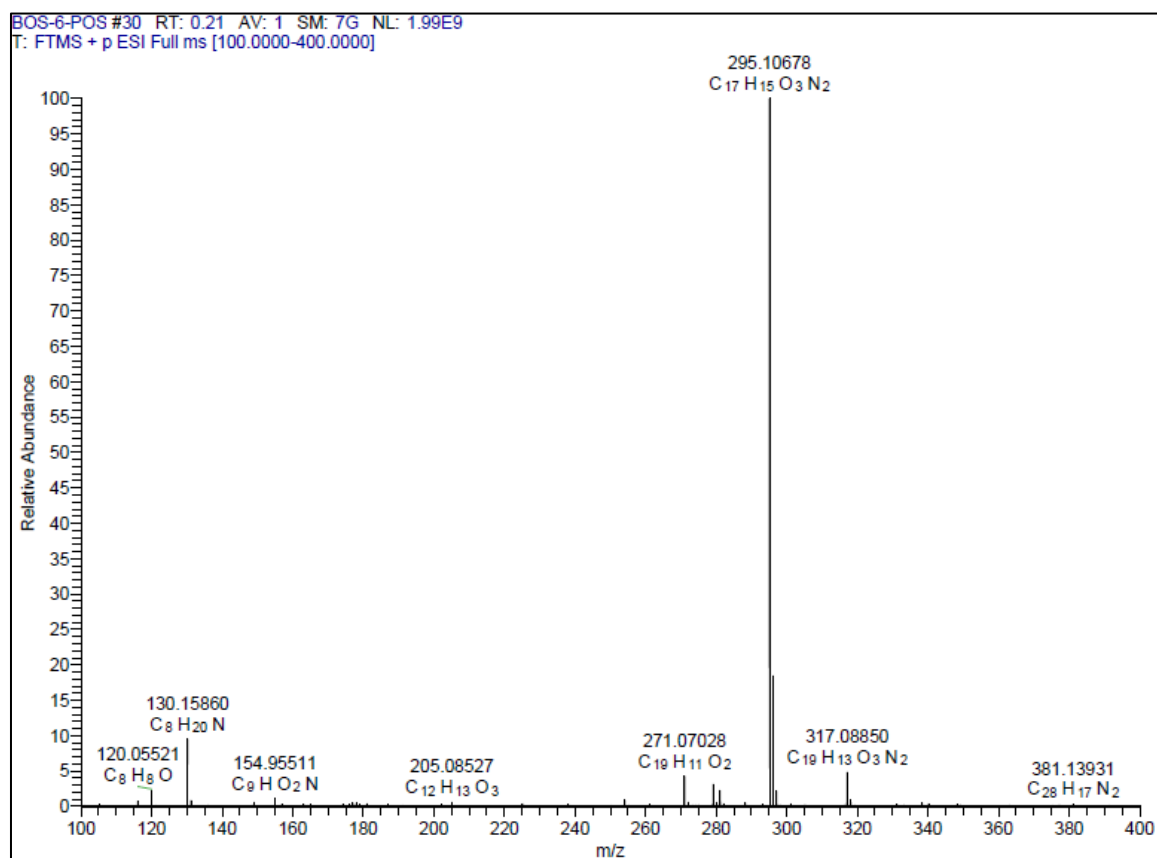
Compound 4



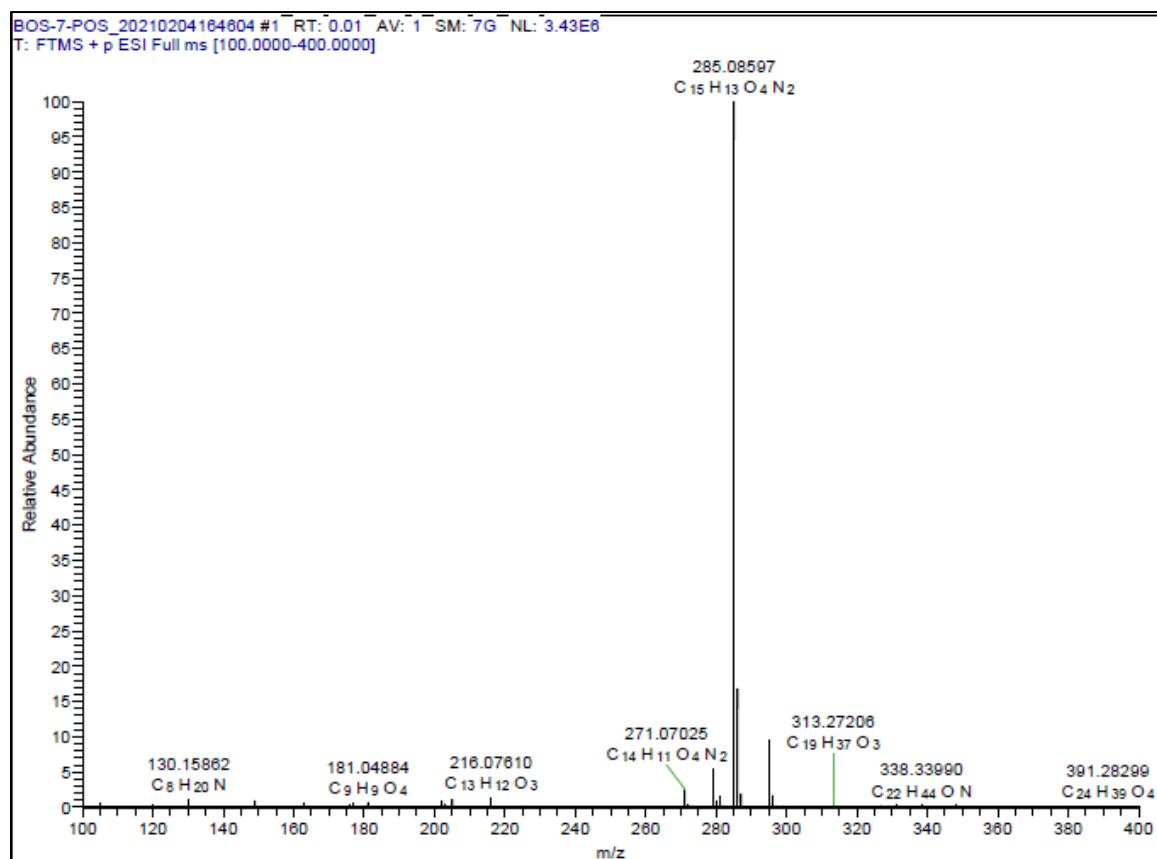
Compound 5



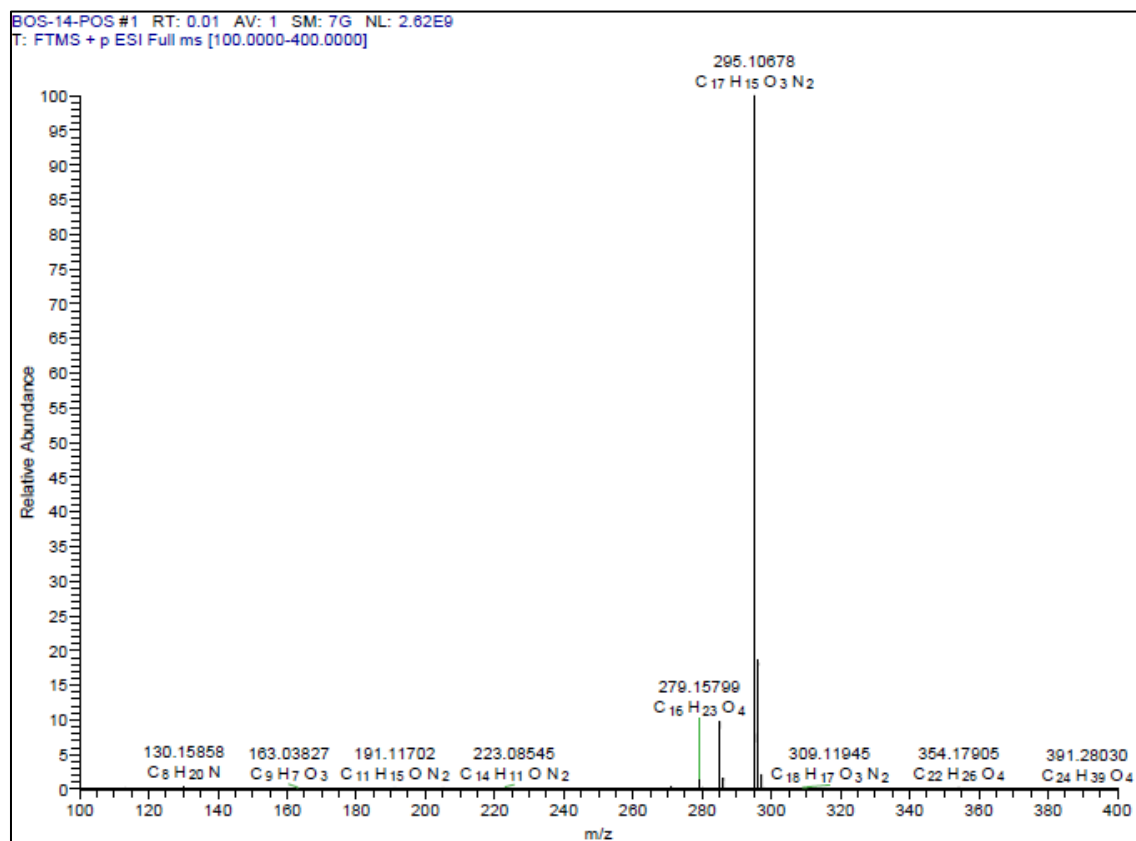
Compound 6



Compound 7



Compound 8



Compound 9

